

# Confidential Prompting: Privacy-preserving LLM Inference on Cloud

Caihua Li\*, In Gim\*, Lin Zhong

Department of Computer Science

Yale University

{caihua.li, in.gim, lin.zhong}@yale.edu

\* Both authors contributed equally

**Abstract**—This paper introduces a vision of *confidential prompting*: securing user prompts from untrusted, cloud-hosted large language model (LLM) provider while preserving model confidentiality, output invariance, and compute efficiency. As a first step toward this vision, we present *Obfuscated Secure Partitioned Decoding* (OSPD), a system built on two key innovations. First, *Secure Partitioned Decoding* (SPD) isolates user prompts within per-user processes residing in a confidential virtual machine (CVM) on the cloud, which are inaccessible for the cloud LLM while allowing it to generate tokens efficiently. Second, *Prompt Obfuscation* (PO) introduces a novel cryptographic technique that enhances SPD’s resilience against advanced prompt reconstruction attacks. Together, these innovations ensure OSPD protects both prompt and model confidentiality while maintaining service functionality. OSPD enables practical, privacy-preserving cloud-hosted LLM inference for sensitive applications, such as processing personal data, clinical records, and financial documents.

## I. INTRODUCTION

Large language models (LLMs) are often hosted on cloud, which introduces privacy concerns as prompts can include sensitive data, ranging from personal communications to health information. Not surprisingly, many IT, healthcare and financial industries, wary of information breaches, restrict the usage of cloud LLM at work [1], [2]. Privacy concerns also subject cloud-hosted LLM serving to regulations like GDPR and HIPAA [3], [4], [5], hampering their adoption. Cloud-hosted LLM serving further raise intellectual property (IP) concerns as prompts are increasingly recognized as IPs with emerging marketplaces. Both privacy and IP concerns underscore the importance of safeguarding prompt confidentiality in cloud environments.

This paper aims at *confidential prompting* in cloud-hosted LLM serving. We assume that **the users and the LLM provider are mutually untrusted**. Each party seeks to uncover the other’s secrets, namely user prompts and LLM weights. Under this assumption, our design secures user prompt confidentiality while achieving three additional crucial goals for commercial deployment: (1) *Model confidentiality* prevents LLM weight leakage to users; (2) *Output invariance* guarantees the LLM responses remain the same regardless of whether security measures are applied or not; (3) *Compute efficiency* requires the introduction of security measures does not significantly increase the service cost.

As outlined in §II-B and §II-D, none of the existing solutions achieve all of our goals under the assumption of an

untrusted LLM. For example, techniques like edge inference [6] protect prompts by processing them locally, which do not work for large models and require sharing weights with users, breaching model confidentiality. Differentially private in-context learning [7], [8] and data anonymization [9], [10], [11], [12] reduce fidelity, violating output invariance. Although fully homomorphic encryption [13], [14] preserves model confidentiality and output invariance, its extensive computation restricts its feasibility for LLMs. More recently, *confidential computing* (CC) [15] has emerged as a promising approach to securing cloud-hosted DNNs [16], [17], [18], particularly via the confidential virtual machines (CVMs) with GPU support. However, existing confidential inferencing approaches with CVM (§II-B2) either require complete trust in the LLM provider or prove inefficient for LLM serving. This inefficiency arises from (i) the lack of batch parallelism and (ii) the large memory footprint of LLMs, severely limiting scalability.

This paper presents a new approach to *confidential prompting*, which delivers LLM serving within a CVM in an efficient and scalable manner, illustrated by Figure 1. It does so without complete trust in the LLM provider. Our key insight is that LLM delivery involves two distinct phases: prefill and decode, where the computation in the latter phase can be formulated as a secure two-party computation. Our approach, called *Obfuscated Secure Partitioned Decoding* (OSPD), performs the prefill phase inside per-user processes and retains the resulting KV attention states (called private KV cache) within these processes. OSPD then performs decode mostly in another dedicated LLM process, without disclosing the private KV cache, using a technique called *Secure Partitioned Decoding* (SPD) (§IV).

SPD formulates token generation (decode) as a secure two-party computation, where one party is a per-user process and the other is the LLM process. In other words, we partition the full attention score computation into two parts: the private and the public attention scores, namely  $A_{\text{pvt}}$  and  $A_{\text{pub}}$ , computed by the two parties respectively. During decode, the user process uses the precomputed private KV cache to compute private attention score  $A_{\text{pvt}}$ , without requiring the LLM weights and thereby reducing the memory footprint. Then it sends  $A_{\text{pvt}}$  to the LLM process. On the other side, the LLM process computes the public attention score  $A_{\text{pub}}$ , merges it with  $A_{\text{pvt}}$  received from the user process for token generation, and maintains

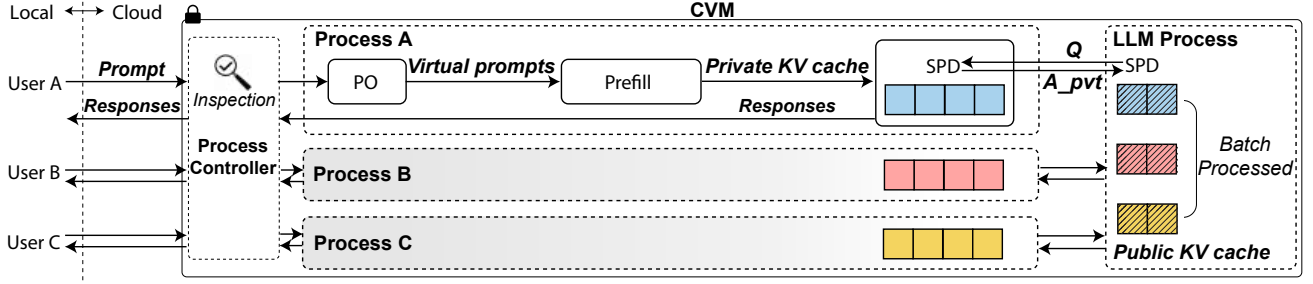


Fig. 1: **OSPD Overview.** A user and its process in the CVM collaborate to protect the user prompt from the LLM provider with Secure Partitioned Decoding (SPD) and Prompt Obfuscation (PO). The user securely sends a prompt to its process. Then the process prepare the virtual prompts and private KV cache before the decoding. SPD involves both the user and the LLM processes. After decoding, the user process sends responses back to the user, subject to inspection by the Process Controller.

public KV cache accordingly.

Our SPD design is secure, efficient and lossless. First, the user prompt and private KV cache remain confidential within the user process. The LLM learns only the private attention score  $A_{pvt}$  and the generated output tokens. The former typically cannot be reversed to the prompt due to the irreversible feature of attention computation. As for the latter, empirical security evaluation in the latest work [19], which systematically tested state-of-the-art prompt stealing techniques on in-the-wild prompts and responses, provides strong evidence that these techniques achieve low prompt recovery rates in practice, indicating that SPD is secure against existing prompt stealing attacks [20], [21], [22]. Second, SPD is efficient because (i) the LLM can batch process public KV cache and attention scores for multiple users in parallel, and (ii) the user processes do not retain LLM weights during decode, thereby maintaining a small footprint. Finally, SPD ensures output invariance as the attention score decomposition is lossless (§IV-B).

Although empirical security evaluation [19] indicates that existing state-of-the-art prompt stealing techniques perform poorly in practice, advanced prompt reconstruction attacks may emerge in the future. To further protect sensitive information in user prompts, such as Personal Identifiable Information (PII), we propose *Prompt Obfuscation (PO)* (§V), which offers an extra layer of protection over sensitive segments. PO generates fake n-grams that appear as authentic as the sensitive segments and uses them to create  $\lambda$  *virtual prompts*, which are processed identically to the original prompt. From an attacker’s perspective, the  $\lambda + 1$  prompts are statistical indistinguishable, rendering the attacker’s advantage negligible beyond random guessing. Only the user can identify the authentic prompt and response. This novel cryptographic design is inspired by *chaffing and winnowing* (§II-C).

PO complements SPD, and together they defend against attacks more effectively than when either technique is employed independently. On one hand, PO obfuscates prompts to defend against the most powerful reconstruction attacks, even in the extreme case where all  $\lambda + 1$  prompts are reconstructed. PO minimizes the risk of leaking sensitive information, as formally proven in §V-B, while enabling SPD to offload the majority of

computation to the untrusted LLM. In other words, PO allows SPD to balance efficiency and scalability with minimal security risk. On the other hand, like many existing obfuscation methods, a knowledgeable attacker with sufficient statistical information about user prompts may compromise PO’s protection. However, SPD prevents the attacker from accurately obtaining the  $\lambda + 1$  prompts, thereby increasing the cost of collecting reliable statistical information and reducing the attacker’s confidence in any data they may collect.

Beyond prompt confidentiality, maintaining model confidentiality is essential for commercial deployment. To address this, OSPD leverages the *Process Controller* and the underlying trusted guest OS to restrict the IO capabilities of the untrusted user processes. After remote attestation and process initialization, OSPD allows these processes to send only the generated output tokens out of the CVM, subject to inspection by the Process Controller. This ensures that the user processes cannot leak the weights via transmitting arbitrary bytes.

In §VIII, we discuss how OSPD collaborates with existing defenses to mitigate attacks out of our threat model, as well as the portability and limitations of OSPD design. For example, although a prompt-leakage injection attack performed by the LLM is out of our Honest-but-Curious (HBC) threat model (see §III-B for details), OSPD can work with existing attention-based detection methods to defend against the attack.

In §VI, we report an implementation of OSPD using PyTorch. In §VII, we evaluate our prototype on an NVIDIA H100 GPU with CC enabled, comparing OSPD with two existing confidential inferencing approaches (§II-B2). We show that OSPD scales well to the number of concurrent users and achieves  $5\times$  better latency than the existing CVM-based approach defending against an untrusted LLM. We conclude our work in §IX, believing that cloud LLM serving that is both privacy-preserving and efficient is important and timely. Our work marks the first step towards utilizing confidential computing for privacy-preserving LLM serving, and we hope it will spark further discussion on confidential prompting. The source code for OSPD can be found at [github.com/yale-sys/confidential-prompting](https://github.com/yale-sys/confidential-prompting).

## II. BACKGROUND AND RELATED WORK

We next provide a succinct background of related techniques.

### A. LLM Inference with KV cache

1) *LLM Inference*: We consider GPT-style LLMs [23], [24], [25], [26], which are trained to predict the distribution of the next token,  $x_{n+1}$ , given a sequence of tokens  $x_1, \dots, x_n$ , known as causal language modeling. This prediction process uses the Transformer architecture [27], which consists of multiple self-attention layers. For a sequence of length  $n$ , represented as  $X \in \mathbb{R}^{n \times d}$ , the Transformer produces an output sequence  $Y \in \mathbb{R}^{n \times d}$ , where  $d$  is the hidden dimension size. The self-attention mechanism requires five matrix multiplications. First, the model computes matrices  $Q = XW_Q$ ,  $K = XW_K$ , and  $V = XW_V$ , where  $W_Q$ ,  $W_K$ , and  $W_V \in \mathbb{R}^{d \times d}$  are trainable weight matrices. Next, the output is calculated as  $Y = \sigma(QK^\top)V$ , where  $\sigma(\cdot)$  denotes the softmax function. The output becomes an input to the next layer. The LLM samples the next token  $x_{n+1}$  from the distribution and appends it to the token sequence, iteratively until some termination condition is met, so called autoregressive token generation.

2) *KV Cache*: The KV cache mechanism [28], [29], [30], [31] is a technique used to improve LLM inference efficiency. This mechanism leverages the causal nature of LLMs: when predicting a token  $x_i$  within a token sequence, the attention computation only considers preceding tokens,  $x_1, \dots, x_{i-1}$ , rather than any tokens that follow. Consequently, instead of recalculating attention for all tokens at each generation step, the LLM inference engine “caches” previously computed attention states and reuses them for subsequent inferences. Since the reusable attention states consist of the  $K$  and  $V$  matrices for each token, this technique is referred to as KV caching.

### B. Confidential Computing and Inferencing

1) *Confidential Computing*: Confidential computing protects data in use, complementing traditional security measures such as encryption that protect data at rest and data in transit. The most common approach to confidential computing is to use trusted execution environments (TEEs), such as enclaves and confidential virtual machines (CVMs), which are provided by hardware features like AMD SEV [32] and Intel TDX [33]. These environments isolate sensitive data and code. Thanks to their strong isolation capabilities, hardware-based TEEs ensure even privileged entities such as the OS and hypervisor cannot access the data being processed. In addition to isolation, most hardware-based TEEs also provide runtime encryption and remote attestation. Runtime encryption guarantees all code and data within a CVM (or enclave) are encrypted in memory, offering an additional layer of protection. Remote attestation allows users to verify the integrity of a remote CVM (or enclave) running in the cloud before transmitting any sensitive data. Originally exclusive to CPUs, confidential computing is now supported by the latest GPUs as well, such as the NVIDIA H100 [34]. Many cloud providers offer confidential computing as a service, primarily through the use of CVMs. In this work, we use the terms TEE and CVM interchangeably.

2) *Confidential Inferencing*: An intuitive approach for applying confidential computing to LLM serving is to serve multiple users with a single LLM instance running in a shared CVM (Figure 2b). This approach is used by most existing commercial services, such as confidential inferencing in Azure [17] and AWS [18]. Although this approach effectively protects against a malicious cloud provider and adversaries that compromise the cloud, it requires all users to fully trust the LLM provider. Even if the LLM provider is trusted, a malicious user may leverage security holes in the LLM software to leak sensitive information from other users’ prompts [35].

An alternative approach is to instantiate a dedicated LLM instance for each user in a separate process (Figure 2c). This setup offers stronger security, as the isolation between user prompts is guaranteed by the OS instead of the LLM software. However, it suffers from two significant inefficiencies: (i) low throughput due to reduced batch parallelism, and (ii) limited scalability as the number of concurrent per-user processes is constrained. For example, a LLM with 13B parameters requires about 26 GB of memory for its weights using 16-bit floating point, which means that a 80 GB GPU can support up to three concurrent user processes. Moreover, inference is performed independently for each of  $m$  users, e.g.,  $X_1W, \dots, X_mW$ , which is less efficient than batching as  $(X_1 : \dots : X_m)W$ .

Our solution, SPD, addresses both challenges by isolating only user prompts in the per-user processes while sharing the LLM among multiple users (Figure 2d). SPD’s goal is not to replace existing solutions, but to offer an alternative approach for different scenarios, as discussed in §VIII-C. Some prior work [36], [37] can enhance isolation between multiple processes within a single CVM, which can be applied together with SPD. However, when used independently, they fail to address the two inefficiencies mentioned above.

### C. Chaffing and Winnowing

In an information-theoretic sense, a message is secure if an eavesdropper can do no better than guessing randomly to determine its content [38], [39]. Modern encryption achieves this by transforming messages into ciphertexts that are indistinguishable from random noise; however, it renders the text meaningless to an LLM. In contrast, *chaffing and winnowing* [40], [41] secures message confidentiality without encrypting the message itself. In naïve chaffing and winnowing, a sender secures sensitive messages by mixing them with fake ones, known as *chaffing*. For example, to secure the message “Meet at 5 pm”, the sender might transmit it along with variations like “Meet at  $T$  pm”, where  $T$  ranges from 1 to 12. Assuming both the sender and the receiver share a symmetric secret key for signing and verifying a message authentication code (MAC) sent along with a message, the receiver can authenticate if a message originates from the sender. The sender includes a fake MAC with each fake message, which enables the receiver to identify and discard fake messages, known as *winnowing*.

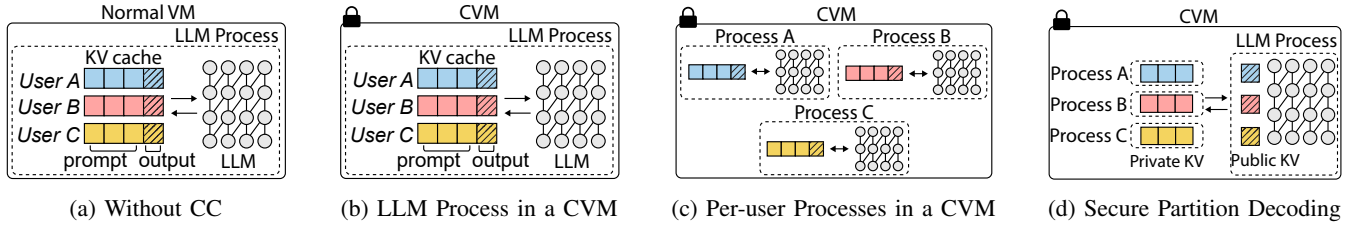


Fig. 2: **Various LLM serving approaches.** (a) LLM serving without confidential computing (CC) is the most efficient, but user prompts and LLM weights are exposed to the cloud provider and any adversaries on the cloud. (b) LLM serving with a LLM process in a CVM protects against the cloud platform, but user prompts are exposed to the LLM provider. (c) A dedicated per-user process offers higher level of protection from both the cloud platform and the LLM provider, but it is inefficient due to lack of batch parallelism and large memory footprint. (d) SPD strikes a balance between security and efficiency by isolating only the user prompts (and private KV cache) within the per-user processes, while allowing batch processing across users.

#### D. Related Work

1) *Prompt Reconstruction*: Prompt stealing attacks [20], [21], [22] aim to recover user prompts from LLM responses. Although these state-of-the-art attacks may succeed on academic prompt datasets, empirical evaluation in the latest work [19] indicates that they perform poorly on in-the-wild prompts in real-world scenarios. Beyond prompt stealing attacks, another novel side-channel attack [35] allows a malicious user to leverage the shared KV cache mechanism, which is common in popular LLM software such as vLLM [42] and SGLang [43], as a side channel to recover prompts of other users.

2) *Privacy-Preserving LLM Inference*: In recent years, researchers have explored various approaches beyond confidential computing to preserve user privacy in LLM inference [44].

*Differential Privacy* protects prompt confidentiality by injecting noise into token distributions [7], [45], generating few-shot random examples [8], or tuning prompts [46]. However, these methods are task-specific and compromise output invariance.

*Multi-Party Computation* (MPC)-based methods utilize *secret sharing* that cryptographically splits a number, either an LLM weight or a prompt token, into multiple numbers. Then they distribute each split to an untrusted party. The user derives the LLM responses by cryptographically combing the outputs of these parties. This technique suffers from multiple problems. First, the untrusted parties must not collude. Second, secret sharing is not efficient for all LLM operations. Recognizing its inefficiency, the authors modify the model, e.g., using ReLU instead of SoftMax [47], or use a much smaller model distilled specially [48], requiring retrain and violating output invariance.

*Homomorphic encryption* (HE) enables computation on encrypted data and is often combined with MPC to secure user privacy in LLM inference [49], [50], [14], [51]. However, its significant overhead impedes its use in real-world applications, particularly for nonlinear functions. Recent works [49], [50], [51] replace these functions with approximations, impeding the use of existing well-trained models.

*Data anonymization* [9], [10], [11], [12] masks or replaces sensitive segments in prompts, such as names and locations. It either fails to protect the secrets or leads to meaningless responses, when the secrets are essential for the task.

*Obfuscation* generates redundant instances, such as privacy-preserving representations [52], pseudo prompts [53], and noise tokens [54], which are mixed with authentic ones to confuse attackers. The key idea is attackers cannot distinguish authentic instances from the faked ones, while users with private prior knowledge can. These approaches share similarities with our design of PO. However, OSPD enhances PO by collaboration with SPD, which seals the entire prompt and private KV cache, thereby increasing the cost of breaking the obfuscation via collecting statistical information.

### III. DESIGN OVERVIEW

We introduce the goals (§III-A) and assumptions (§III-B) of OSPD, and an overview of the design (§III-C).

#### A. Design Goals

Our primary goal is to secure user prompt confidentiality in cloud-hosted LLM serving. Beyond the primary goal, we target three additional goals for commercial deployment.

- **Model confidentiality**: LLM weights must not be leaked. This is critical as the weights constitute an intellectual property of the LLM provider. Preserving model confidentiality enhances the deployability to close-source LLMs.
- **Output invariance**: Security measures must not change the output of LLM. We believe it is crucial for deployment, particularly for tasks in clinical and financial fields, where even a small accuracy error could lead to serious consequences.
- **Compute efficiency**: Security measures cannot significantly increase the cost. While security is not free, we believe that a more efficient approach is more attractive to users.

#### B. Trust and Threat

We categorize all parties into four categories: (1) users, (2) LLM provider, (3) cloud provider, (4) hardware and guest software stack providers, such as Nvidia and Linux community.

**Trusted Computing Base (TCB)** Our TCB includes the CPUs and GPUs hardware in the cloud, as well as the software stack in a CVM like Linux kernel and Nvidia CUDA stack. We trust the architectural extensions of confidential computing, such as AMD SEV [32], Intel TDX [33], and Nvidia GPU CC [34].

Users and LLM provider verify the integrity of CVM in cloud via remote attestation (§II-B1) before sending any secrets.

In contrast, the cloud provider may be malicious or the cloud platform may be compromised, and thus it is out of the TCB. In addition, the users and the LLM provider are also excluded from the TCB, as they are mutually untrusted, which means they may attempt to uncover each other’s secrets.

We assume the communication between users (or LLM provider) and their associated processes in the CVM are secure. We also assume the users and their processes privately share the keys (or seeds) for pseudorandom functions (PRFs).

**Threat Model** Based on the above trust model, we consider the following three kinds of threats:

- **Cloud Provider Threat:** The malicious cloud provider or any adversaries that compromise the cloud platform attempt to steal user prompts and LLM weights.
- **LLM Provider Threat:** The LLM provider, possibly colluding with users, attempts to steal other user prompts.
- **User Threat:** A user leverages security holes in LLM software to steal LLM weights and other user prompts.

For example, the solution depicted in Figure 2a is vulnerable to all three kinds of threats, while the solution depicted in Figure 2b is threatened by the LLM provider and the user [35].

Although the LLM provider is untrusted, being curious about user prompts and potentially seeking profit from user secrets, we believe the provider is rational. As a result, we assume that the LLM strictly follows the prescribed inference steps, following the Honest-but-Curious (HbC) threat model. This assumption is reasonable because our design technically enforces that the LLM cannot access user prompts. While a malicious LLM may alter the generation to induce prompt leakage, such misbehaviors are detectable. In other words, our design prevents the LLM provider from stealing secrets without risk of detection, such as accessing plaintext prompts in memory. This distinguishes our attack surface from traditional cloud-hosted LLM serving, aligning our Honest-but-Curious threat model with real-world incentives. To defend against a stronger threat model, please refer to our discussion in §VIII-A.

We do not consider attacks that compromise the CVM, the communication channels, or the pseudorandom function (PRF). Denial of service (DoS) attacks are out of scope in this work.

### C. OSPD Overview

OSPD targets all the goals in §III-A. As depicted in Figure 1, its core components, *Secure Partitioned Decoding (SPD)* and *Prompt Obfuscation (PO)*, collaborate to defend against threats in §III-B. We next provide an overview of this collaboration.

**Initialization** Assuming that all users and the LLM provider achieve a consensus on the trusted guest software stack, e.g., Linux kernel and Nvidia CUDA stack, one party creates a CVM in the cloud, while all parties verify its integrity via remote attestation. Then users and LLM provider communicate with the Process Controller in the CVM to create their associated processes, and transmit their secrets, i.e., user prompts and LLM weights, over secure communication channels.

**Prompt Obfuscation (§V)** PO has two steps to generate *virtual prompts*: (1) tagging sensitive segments within a prompt and (2) sampling fake n-grams for each tagged segment.

For (1), we can leverage any existing tool or allow a user to provide a customized small language model (SLM) to automatically tag sensitive segments in a prompt. For simplicity, we use Google’s PII detection tool to tag Personally Identifiable Information (PII) as an example.

For (2), a user process handles each tagged sensitive segment  $S_{\text{tag}}$  in a prompt  $S_0$  independently (§V-A). That is, the process samples a set of fake n-grams  $F$ , such that for each  $S_{\text{fake}} \in F$ ,

$$|\ln(LM(S_{\text{fake}}|S_0/S_{\text{tag}})) - \ln(LM(S_{\text{tag}}|S_0/S_{\text{tag}}))| \leq \epsilon, \quad (1)$$

where  $\ln$  is the natural logarithm,  $\epsilon$  is an error bound parameter, operation  $S_a/S_b$  denotes replacing segment  $S_b$  with empty slots in  $S_a$ , and  $LM(S)$  represents the probability of the given token sequence  $S$  estimated by the language model  $LM$ .

The user process generates  $\lambda$  *virtual prompts* with  $F$ , which are statistical indistinguishable from the original prompt, and generates a number  $idx$  with a pseudorandom function (PRF), serving as the index of the authentic prompt in  $\lambda + 1$  prompts.

**Prefill (§IV-A)** The user process computes *private KV cache* for all  $\lambda + 1$  prompts, always keeping these prompts and their private KV cache within the user process without any exposure.

We note that the user process requires LLM weights for the computation during prefill. After initialization, OSPD disallows user processes to send any data out of the CVM, except the generated output tokens. The trusted Process Controller inspects all outbound data to avoid LLM weights leakage, thereby ensuring *model confidentiality*.

**Secure Partitioned Decoding (§IV-B)** SPD formulates the attention score computation during decode phase into a two-party computation. That is, the user process and the LLM computes the private and the public attention scores respectively. Specifically, the private attention score  $A_{\text{pvt}}$  is computed with the private KV cache, which is precomputed during prefill and stored in the user process. Consequently, it does not require the LLM weights for computation during decode. This minimizes the footprint during decode and enables greater scalability.

After computation, the user process sends  $A_{\text{pvt}}$  to the LLM, which then merges the received  $A_{\text{pvt}}$  with the public attention score  $A_{\text{pub}}$  to get the full attention score. As the attention score decomposition is lossless, SPD allows the LLM to generate tokens while maintaining *output invariance*.

In addition, SPD achieves *compute efficiency* as it allows the LLM to batch process prompts of multiple users, and the footprint of user processes remains small during decode.

**Complementarity between SPD and PO** SPD and PO are complementary techniques that collaboratively defend against attacks more effectively than when either technique is employed independently. On one side, although empirical evaluation indicates SPD is resilient against state-of-the-art prompt stealing attacks [19], it may still be vulnerable to advanced prompt reconstruction attacks that may emerge in the future. On the other side, attackers can improve their chances of defeating



PO by obtaining detailed knowledge about the distribution of virtual prompt generation through statistical analysis.

However, these attacks breach OSPD only at a high cost and with a low probability of success. All  $\lambda + 1$  prompts and their private KV cache securely reside within the user process. The protection provided by SPD significantly increases the cost of collecting statistical information, e.g., reconstruction via approximation, and reduces the confidence level of any statistical analysis. Even in the worst-case scenario where an adversary reconstructs all  $\lambda + 1$  prompts, the adversary gains only marginal advantage in breaching PO than random guessing among the  $\lambda + 1$  possible prompts, as formally proven in §V-B.

**Extract Authentic Response** The user process sends all  $\lambda + 1$  responses to the user. It is worth noting that the user already knows the index  $idx$  of the authentic response, as we assume the user and its process share the key of the PRF (§III-B). This allows the user to extract the authentic response.

#### IV. EFFICIENT PROMPT PROTECTION WITH CONFIDENTIAL COMPUTING

Keeping dedicated copies of LLM weights in per-user processes leads to significant inefficiency as discussed in §II-B2. This is the main obstacle to use per-user processes for LLM serving while untrusting the LLM provider. We solve this challenge by eliminating the need to retain LLM weights in user processes after the initial prefill phase. Our key insight is the decoding can be formulated as a secure multi-party computation, with each user process being one party that does not need access to the LLM weights. We partition KV cache into *private* and *public* parts. The KV cache of a user prompt is private and kept confidential in the process, while that of the generated tokens is public to the LLM. For simplicity, we detail the protocol in a single-user scenario, assuming the CVM and processes have been verified and initialized, and PO (§V) is not applied.

There are three participants in the protocol: (i) a user; (ii) the user's process; and (iii) the LLM.

- 1) **Prefill** (§IV-A): A user sends an encrypted prompt to its process in the CVM, which then decrypts the prompt, computes private KV cache  $K_{Pvt}, V_{Pvt}$ , generates the first token, and finally sends the first token to the LLM.
- 2) **Decode** (§IV-B): As in Figure 3, for each transformer layer:
  - a) The LLM computes  $Q_{New}, K_{New}, V_{New}$  of the received token, sends  $Q_{New}$  to the user process, and appends  $K_{New}, V_{New}$  to public KV cache  $K_{Pub}, V_{Pub}$ .
  - b) The user process responds with private attention score  $A_{pvt} = \sigma(Q_{New} K_{Pvt}^T) V_{Pvt}$ .
  - c) The LLM computes public attention score  $A_{pub} = \sigma(Q_{New} K_{Pub}^T) V_{Pub}$ , merged with  $A_{pvt}$  to recover full attention score  $Y = \sigma(Q_{New} K^T) V$  via Theorem 1.
  - d) If it is the final layer, send output  $Y$  to the user process.
- 3) The user process samples a new token from  $Y$  and sends it to the LLM and the user. Then go to Step 2 until [EOS].

This protocol can be generalized to scenarios with multiple users, each with its own process operating in the CVM.

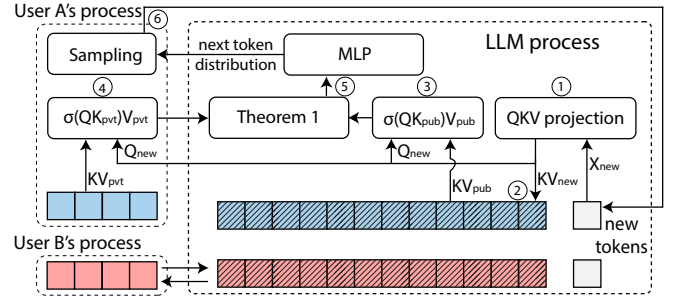


Fig. 3: **Overview of SPD** on a simplified Transformer layer. The squares with varying colors represent the KV cache associated with different users. ① Project hidden state  $X_{new}$  of a new token to  $Q_{new}, K_{new}, V_{new}$ . ② Append  $K_{new}, V_{new}$  to the public KV cache. ③ Batch process public attention score for all users. ④ Compute private attention score in each user process. ⑤ Merge results to compute full attention score and return the next token distributions to user processes. ⑥ Sample the next token then repeat until finish.

##### A. Prefill in CVM

Upon receiving the  $n$ -token prompt from the user, the user process computes private KV cache  $K_{Pvt}, V_{Pvt} \in \mathbb{R}^{n \times d}$ , generates the first token and sends it to the LLM.

**Security Analysis of Model Confidentiality** The user process requires read-only access to the LLM weights for computation during the prefill phase. Although it obtains the LLM weights, it is permitted to send only the generated output tokens out of the CVM. The Process Controller inspect outbound data to enforce this restriction, thereby preventing the leakage of LLM weights to the user. Details of the enforcement are in §VI.

We note that even the deployment of PO (§V) does not require the user process to send any data other than the generated output tokens. Sending any additional data to the user after initialization could potentially leak LLM weights. In particular, after initialization, both the user and its process can independently determine the index of the authentic response among the  $\lambda + 1$  candidates, since they share the key of the PRF (§III-B) and thus require no further communication.

##### B. Secure Partitioned Decoding (SPD)

We formulate the decoding as a secure two-party computation based on the online softmax calculation [55]. This approach allows the LLM to retrieve the full attention score  $Y$  without knowing the private KV cache  $K_{Pvt}$  and  $V_{Pvt}$ .

**Theorem 1** (Secure Two-party Attention Computation). *Let  $Q \in \mathbb{R}^d$ ,  $K = \text{concat}(K_{Pvt}, K_{Pub}) \in \mathbb{R}^{n \times d}$ ,  $V = \text{concat}(V_{Pvt}, V_{Pub}) \in \mathbb{R}^{n \times d}$ , and  $\sigma$  be the softmax function.*

$$\sigma(QK^T)V = \frac{\gamma_{Pvt}}{\gamma_{Pvt} + \gamma_{Pub}} \sigma(QK_{Pvt}^T)V_{Pvt} + \frac{\gamma_{Pub}}{\gamma_{Pvt} + \gamma_{Pub}} \sigma(QK_{Pub}^T)V_{Pub}, \quad (2)$$

where  $\gamma_{Pvt}, \gamma_{Pub}$  are denominators of each softmax operation, e.g.  $\gamma_{Pvt} = \sum \exp(QK_{Pvt}^T)$ .

Theorem 1 is lossless and its proof is available in §A. This theorem serves as the foundation for the SPD design, which offers two key benefits. First, the LLM can batch process all public states  $(Q, K_{\text{Pub}}, V_{\text{Pub}})$  of multiple users in parallel. Second, computations in user processes have a fixed cost and do not involve LLM weights, allowing the user processes to retain only a small amount of memory for the private states. In addition, SPD only induces a constant communication overhead of  $2d + 1$  floating points in each round. We note that computing  $\gamma_{\text{Pvt}}$  and  $\gamma_{\text{Pub}}$  individually is numerically unstable due to its exponential term. Instead, we compute  $\gamma_{\text{Pvt}} = \sum \exp(QK_{\text{Pvt}}^\top - m_{\text{Pvt}})$ , where  $m_{\text{Pvt}} = \max(QK_{\text{Pvt}}^\top)$ . The coefficients in Theorem 1 become  $\gamma_{\text{Pvt}}/(\gamma_{\text{Pvt}} + \alpha\gamma_{\text{Pub}})$  and  $\gamma_{\text{Pub}}/(\alpha^{-1}\gamma_{\text{Pvt}} + \gamma_{\text{Pub}})$ , where  $\alpha = \exp(m_{\text{Pub}} - m_{\text{Pvt}})$ .

### C. Security Analysis

We analyze the security of SPD according to the sources of threats outlined in §III-B.

First, user prompts and LLM weights remain confidential from the cloud provider and any adversaries on the cloud. These secrets are transmitted to the CVM over secure channels only after the CVM integrity is verified via remote attestation. Attacks that compromise the CVM or its guest OS are out of scope of this work and we discuss these attacks in §VIII-A.

Second, the LLM cannot access user prompts as the prompts and their private KV cache remain confidential within per-user processes. The trusted guest OS guarantees isolation among processes to avoid any secret exposure. The LLM learns only (1) the generated output tokens, and (2) the private attention score  $A_{\text{Pvt}}$ . However, it is not practical for an attacker to recover user prompts from such information. For (1), the state-of-the-art techniques for recovering prompts from LLM responses [20], [21], [22] have been proven to perform poorly on in-the-wild prompts in practice [19]. For (2), the attention score computation is an information-losing map. It filters out much information about the prompt and retains only information that is relevant to the output token generation, as its name “attention” suggested. As a result, the private attention score  $A_{\text{Pvt}}$  is typically irreversible to the user prompt, unless the query matrix  $Q$  is adversarially selected. This implies that a more promising attack is to inject prompt-leakage instructions, which induce the private attention score to keep as much information about the prompt as possible, and further induce prompt leakage in token generation. However, such an attack would require the LLM to manipulate the inference process, increasing the risk of detection and falling outside our Honest-but-Curious threat model. We discuss the detection of prompt-leakage injection attacks via tracking attention scores in §VIII-A.

Finally, the users cannot obtain other users’ prompts or LLM weights because only the generated output tokens are sent out of the CVM. Particularly, side-channel attacks that exploit the shared KV cache mechanism in LLM software [35] cannot succeed with SPD design. This is because SPD relies on the underlying trusted guest OS, rather than the LLM software, to enforce isolation among user prompts and private KV cache.

## V. PROMPT OBFUSCATION

We introduce *Prompt Obfuscation (PO)*, a novel defense mechanism against advanced prompt reconstruction attacks that may emerge in the future. Inspired by *chaffing and winnowing* (§II-C) [40], [41], PO aims to minimize the probability of the LLM provider successfully obtaining the authentic user prompt and response, at the intentional cost of generating redundant tokens for obfuscation. The premise of chaffing and winnowing is twofold: (1) an eavesdropper cannot distinguish authentic messages from fake ones based on their content, while (2) the receiver with private prior knowledge can. PO achieves (1) by leveraging the advanced language model for infilling and (2) by exploiting the private key shared between the user and its process for a pseudorandom function (PRF).

To bewilder attackers and protect sensitive information in a prompt, the user process first tags sensitive segments in the prompt. We can deploy existing tools, such as Google’s PII detection, or allow the user to provide a customized small language model to automate the tagging. The process then generates  $\lambda$  *virtual prompts* by replacing the sensitive segments with sampled fake n-grams. Figure 12 in §E provides an example for illustration. These  $\lambda$  virtual prompts, along with their KV cache, reside within the user process exclusively, in the same way as the authentic prompt and its private KV cache. The user process and the LLM collaborate to decode all  $\lambda + 1$  prompts in parallel with SPD. The LLM is unable to distinguish the authentic prompt from the virtual ones. Even in the worst-case scenario where an attacker breaks SPD and reconstructs all the prompts, all these prompts are guaranteed to be statistically indistinguishable. Only the user and its process know which prompt and response are authentic, as they know the associated index among the  $\lambda + 1$  candidates.

### A. Virtual Prompt Generation

We present *Greedy Quantized Sampling (GQS)*, a simple algorithm designed to sample fake n-grams given a user prompt  $S_0$ , as illustrated in Algorithm 1. We assume the automatic tagging tool marks sensitive segments, i.e., sensitive token subsequences, with `<redacted/>` tags. For simplicity, we assume that the sensitive segments within a prompt are independent and the user process handles them one by one, denoted  $S_{\text{tag}}$ . A tagged segment  $S_{\text{tag}}$  may represent a name, location, medical condition, or other sensitive information. The goal of GQS is to sample fake n-grams, i.e., replacement subsequences, appearing as authentic as the  $S_{\text{tag}}$ . Beyond user prompt  $S_0$  and the tagged segment  $S_{\text{tag}}$ , GQS requires security parameters  $\epsilon$  and  $\lambda_{\text{max}}$ , as well as a pre-trained language model  $LM$ . For brevity, we denote the algorithm as  $GQS(S_0, S_{\text{tag}}, \epsilon)$  while omitting  $\lambda_{\text{max}}$  and  $LM$  from the notation.

GQS leverages the language model  $LM$  to fill in the missing subsequence in a prompt. Specifically, it replaces the tagged segment  $S_{\text{tag}}$  with a fake n-gram  $S_{\text{fake}} \in F$ . Some LLMs are trained for infilling tasks [56], [57], [58]. It has also been shown that simple autoregressive LLMs can perform infilling when the prompts are appropriately formatted [59]. That is, Algorithm 1 uses the *Format* function to generate the formatted prompt

---

**Algorithm 1** Greedy Quantized Sampling (GQS) for Prompt Obfuscation
 

---

**Require:** User prompt  $S_0$  as token sequence, tagged segment  $S_{\text{tag}}$  as sensitive token subsequence, security parameters  $\epsilon$  and  $\lambda_{\text{max}}$ .  $LM$  is a pre-trained language model and  $\{Ctri_i\}$  are the associated pre-defined control sequences used to format the prompt.

```

1:  $S_{\text{context}} \leftarrow S_0 / S_{\text{tag}}$                                 ▷ Replace  $S_{\text{tag}}$  in  $S_0$  with empty slots
2:  $n \leftarrow |S_{\text{tag}}|$                                           ▷ Get the number of tokens in  $S_{\text{tag}}$ 
3:  $\tilde{S} \leftarrow \text{Format}(\{Ctri_i\}, S_{\text{context}}, n)$               ▷ Format the prompt for infilling
4:  $\epsilon' \leftarrow \epsilon / n$                                           ▷ Set the width of each quantized bin as  $\epsilon' = \epsilon / n$ 
5:  $F \leftarrow \{\dots\}$                                           ▷ Initialize the set of fake n-grams (length of 0) with an empty sequence
6: for  $len \leftarrow 1$  to  $n$  do
7:    $F_{\text{new}} \leftarrow \{\}$                                        ▷ Initialize the set of fake n-grams (length of  $len$ ) as an empty set
8:    $X_{\text{ref}} \sim LM(\tilde{S} + S_{\text{tag}}^{1\dots len-1})$                 ▷ Get the distribution of next token when fill in  $S_{\text{tag}}^{1\dots len-1}$ 
9:    $\rho \leftarrow P(X_{\text{ref}} = S_{\text{tag}}^{len})$                         ▷ Get the reference probability  $\rho$  when fill in  $S_{\text{tag}}^{1\dots len}$ 
10:  for each  $S_{\text{fake}} \in F$  do                                     ▷ Iterate over all fake n-gram candidates with length of  $len - 1$ 
11:     $X \sim LM(\tilde{S} + S_{\text{fake}})$                                 ▷ Get the distribution of next token when fill in  $S_{\text{fake}}$  with length of  $len - 1$ 
12:     $F_{\text{new}} \leftarrow F_{\text{new}} \cup \{S_{\text{fake}} + x \mid \lfloor \frac{\ln \rho}{\epsilon'} \rfloor \cdot \epsilon' \leq \ln(P(X = x)) < (\lfloor \frac{\ln \rho}{\epsilon'} \rfloor + 1) \cdot \epsilon'\}$   ▷ Select tokens in the same quantized bin as  $\rho$ 
13:  end for
14:   $F \leftarrow \text{top-}\lambda_{\text{max}}(F_{\text{new}})$                         ▷ Select the top  $\lambda_{\text{max}}$  candidates to keep the compute cost stable
15: end for
16: return  $F$ 

```

---

$\tilde{S}$ , where the sequences  $\{Ctri_i\}$  refer to predefined control sequences used to format the prompt, which are determined by the chosen language model  $LM$ . For example, tokens like <prefix> and <suffix> are commonly used in fill-in-the-middle (FIM) models [60].

GQS requires two security parameters that respectively control the quality and the number of fake n-grams to sample:  $\epsilon \geq 0$  and  $\lambda_{\text{max}} \in \mathbb{N}$ . Parameter  $\epsilon$  is the error bound for the fake n-grams, while parameter  $\lambda_{\text{max}}$  sets the maximum number of candidates to consider. These parameters are adjustable according to security requirements and desired utility.

The user process samples a set of fake n-grams  $F$  with GQS and generates  $\lambda$  virtual prompts by replacing  $S_{\text{tag}}$  with  $S_{\text{fake}} \in F$ . To ensure a minimum level of obfuscation and prevent information leakage when too few virtual prompts can be generated, the user can provide a parameter,  $\lambda_{\text{min}}$ . If fewer than  $\lambda_{\text{min}}$  virtual prompts are generated, the process stops the inference and alerts the user of a potential information leak.

In the case where a prompt contains multiple sensitive segments, since conditioning the fake n-grams on all segments simultaneously is impractical due to the exponential growth in the number of candidates, we process each tagged segment independently. Fake n-grams are sampled for each segment in parallel using GQS. Under the assumption of independence, the total error bound  $\epsilon$  for virtual prompts is given by the sum of the individual error bounds  $\epsilon_j$  for each of the  $j$ -th segment.

### B. Security Analysis

In this section, we formally analyze the probability of PO being compromised. This formal analysis underscores the complementary nature of SPD and PO, aligning with our informal analysis in §III-C.

**Security Model** The key to the security analysis of PO lies in *quantifying the “authenticity”* of virtual prompts. Let  $P$  represent the true language distribution, where  $P(S)$  denotes the probability of  $S$  being an authentic prompt. Denoting the original user prompt as  $S_0$  while the  $\lambda$  virtual prompts as

$S_1, S_2, \dots, S_\lambda$ , if a virtual prompt  $S_i$  satisfies  $P(S_i) = P(S_0)$ , we say that  $S_i$  is as authentic as the original prompt  $S_0$ . In the following, we use the minimal  $C \geq 1$  satisfying

$$\frac{1}{C} \leq \frac{P(S_i)}{P(S_0)} \leq C, \quad \text{for } i = 1, \dots, \lambda, \quad (3)$$

to represent the authenticity of  $\lambda$  virtual prompts, where  $C$  closer to 1 indicates better authenticity.

However, generating  $\lambda$  virtual prompts that are exactly as authentic as the original (i.e.,  $C = 1$ ) is not always feasible for two reasons: (1) such virtual prompts may not exist, and (2) the true distribution  $P$  is unknowable. Instead, PO leverages GQS (Algorithm 1) to generate  $\lambda$  virtual prompts satisfying

$$e^{-\epsilon} \leq \frac{LM(S_i)}{LM(S_0)} \leq e^\epsilon, \quad \text{for } i = 1, \dots, \lambda. \quad (4)$$

The proof of Equation 4 is provided in §B. This indicates that the ratio of probabilities between the virtual prompts and the original prompt, as estimated by the language model  $LM$ , is bounded by the error bound security parameter  $\epsilon$  to GQS.

To quantify the distance between language model  $LM$  and the true language distribution  $P$ , we assume there exists  $\delta \geq 0$  satisfying

$$e^{-\delta} \leq \frac{P(S)}{LM(S)} \leq e^\delta, \quad \text{for } \forall S. \quad (5)$$

As a result, we have

$$e^{-\epsilon-2\delta} \leq \frac{P(S_i)}{P(S_0)} \leq e^{\epsilon+2\delta}, \quad \text{for } i = 1, \dots, \lambda. \quad (6)$$

The proof of Equation 6 is in §C, which indicates the authenticity of virtual prompts is jointly bounded by  $\epsilon$  and  $\delta$ . As both  $\epsilon$  and  $\delta$  approach 0, the  $\lambda + 1$  prompts are statistical indistinguishable, meaning the virtual prompts are nearly as authentic as the original.

**Attack Scenario** We consider an attack scenario in which an adversary breaks SPD and obtains  $\eta$  out of the  $\lambda + 1$  prompts, where  $0 \leq \eta \leq \lambda + 1$ . We assume that the



adversary knows the true language distribution  $P$ , although this assumption is not realistic in practice. The adversary leverages its knowledge of  $P$  to guess one of the  $\eta$  obtained prompts as the original prompt. To be more precise, denoting the  $\eta$  obtained prompts as  $S_{idx_1}, S_{idx_2}, \dots, S_{idx_\eta}$ , the adversary chooses  $S_{idx_i}$  with a probability of  $P(S_{idx_i}) / \sum_{j=1}^{\eta} P(S_{idx_j})$ . However, the original prompt is equally likely to be any of the  $\lambda + 1$  prompts, which means it is possible that none of the  $\eta$  obtained prompts is the original one. We analyze the adversary’s success probability as follows.

The probability that the  $\eta$  obtained prompts include the original prompt is  $\eta/(\lambda + 1)$ . In this case, the probability of the adversary correctly guessing the original prompt satisfies

$$\frac{1}{1 + (\eta - 1)e^{\epsilon + 2\delta}} \leq \frac{P(S_0)}{\sum_{j=1}^{\eta} P(S_{idx_j})} \leq \frac{1}{1 + (\eta - 1)e^{-\epsilon - 2\delta}}. \quad (7)$$

The proof of Equation 7 is provided in §D. As a result, the lower and upper bounds of the success probability are respectively

$$\frac{\eta}{\lambda + 1} \cdot \frac{1}{1 + (\eta - 1)e^{\epsilon + 2\delta}} \text{ and } \frac{\eta}{\lambda + 1} \cdot \frac{1}{1 + (\eta - 1)e^{-\epsilon - 2\delta}}.$$

There are a few cases worth emphasizing. First, when the adversary obtains only one prompt (i.e.,  $\eta = 1$ ), the success probability is  $1/(\lambda + 1)$ , which is equivalent to random guessing without any advantage. Second, when the adversary obtains all the prompts (i.e.,  $\eta = \lambda + 1$ ), the success probability lies between  $1/(1 + \lambda e^{\epsilon + 2\delta})$  and  $1/(1 + \lambda e^{-\epsilon - 2\delta})$ .

This result highlights the complementary nature of SPD and PO. First, without SPD (i.e.,  $\eta = \lambda + 1$ ), an adversary succeeds with the highest probability at almost zero cost. Second, without PO (i.e.,  $\lambda = 0$ ), an adversary succeeds with high confidence at the cost of reconstructing only one prompt.

**Suggestions for Fully Utilizing PO** The above analysis reveals that when advanced prompt reconstruction attacks compromise SPD and obtain all  $\lambda + 1$  prompts, the security of PO depends on three factors: (1)  $\lambda$  as the number of virtual prompts; (2)  $\epsilon$  as the error bound of sampling; and (3)  $\delta$  as the distance between the language model  $LM$  and the true language distribution  $P$ .

In common cases,  $LM$  well captures  $P$ , meaning  $\delta$  approaches 0. An example is when the number of replacement segments is finite and enumerable, such as phrases “I live in [CITY]” and “I am [AGE] years old”. In such cases, PO secures the sensitive segments with a reasonably small  $\epsilon$  and a sufficiently large  $\lambda$ . Empirical evaluation results are in §VII-A.

However, PO may not fully secure the sensitive segments when  $\delta$  increases. This can happen when the language model  $LM$  is not sufficiently well-trained. For example, if the user prompt  $S_0$  contains domain-specific terms or phrases that are not well-represented in the training data of  $LM$ , the model may not accurately estimate the probabilities of these terms. In such cases, PO serves only as an *obfuscation*, as its name suggests, increasing the cost of cryptanalysis and reducing the confidence of attackers, instead of fully securing the secrets. We suggest that users should choose or further fine-tune a

language model that well captures  $P$  on the domain of their prompts to minimize  $\delta$ .

Another scenario where PO does not perform well is when the user prompt  $S_0$  is highly atypical, for example, when  $S_0$  contains syntax errors. In such cases, it may be impossible to generate replacement segments without using a large  $\epsilon$  or a small  $\lambda$ . To prevent potential information leakage, we suggest that users should configure the desired  $\epsilon$  with a minimum value for  $\lambda$ , that is  $\lambda_{\min}$ . When  $\lambda < \lambda_{\min}$ , the process stops the inference and alerts the user.

Finally, the security of PO also depends on if an adversary can obtain the index of the authentic prompt among the  $\lambda + 1$  candidates. We suggest that the user should always keep the index and the key to the pseudorandom function (PRF) private. As stated in §III-B, attacks on the PRF are out of scope.

## VI. IMPLEMENTATION

Consistent with the design (Figure 1), our prototype consists of three main components: the Process Controller, the LLM Server, and the Prompt Vault. During runtime, the LLM Server and the Prompt Vault operate as the LLM and user processes respectively. We implement both the LLM Server and the Prompt Vault using PyTorch, targeting the widely adopted Llama [26] series of open-source LLMs. We next describe key implementation details of our prototype.

**Process Controller** The Process Controller must (1) restrict IO capabilities and (2) inspect outbound data of user processes. It leverages Linux namespaces to achieve (1). That is, it sets the `CLONE_NEWNET` flag in clone system calls when creating user processes. This isolates the user processes from the host network, preventing them from exfiltrating any data via network IO. To send output tokens, a user process can only send to the Process Controller via a pipe, which then inspects and forwards the tokens to the associated user. As for (2), the Process Controller inspects the tokens by comparing them against those of the LLM process. We note that according to our SPD design, the LLM knows the output matrix  $Y$  and thus it knows the groundtruth output tokens.

**LLM Server** We develop the LLM Server based on the Transformers library [61]. To support SPD, we adapt the Llama model by monkey-patching its attention module. We modified the attention score computation to prioritize the computation of matrix  $Q$ , which is sent to each user process asynchronously via the GLOO communication backend [62]. While the server asynchronously waits for all private attention scores to arrive, it continues to compute matrix  $K$ ,  $V$  and public attention scores. Once all scores are ready, it computes the final attention scores with Theorem 1. We note that the GLOO [62] backend transfers tensors via the host, which incurs non-trivial overhead (See §VII-B2). We discuss why other popular communication backends, e.g., NCCL [63], are not suitable in §VIII-B.

**Prompt Vault** The Prompt Vault handles operations including PO, prefill, and private attention score computation. Given a user prompt with tagged segments, the Prompt Vault generates virtual prompts as described in Algorithm 1 and §V. Then it

performs the prefill operations for all the prompts in parallel, preparing the private KV cache as normal. During decoding, the Prompt Vault blocks and waits for the query matrix  $Q$  over the GLOO backend [62]. Once it receives the matrix, it computes the private attention scores based on Theorem 1 and returns the scores to the LLM Server.

## VII. EVALUATION

For empirical security evaluation on prompt stealing attacks, which attempt to recover user prompts from LLM responses, we refer to the analysis in previous work [19] (§II-D1). In this section, we primarily aim to answer two additional questions:

- Can PO preserve sensitive information in practice?
- Does OSPD maintain compute efficiency?

To answer the first question, we empirically examine (1) the maximum available  $\lambda$  for the desired error bound  $\epsilon$ , and (2) the effect of other factors that influence the sampling. After that, we evaluate the performance of OSPD compared to two existing confidential inferencing approaches (§II-B2).

**Evaluation setup** Without special mention, all evaluations were conducted in a CVM on Azure, i.e., the *NCCads\_H100\_v5* [64]. The CVM is equipped with an NVIDIA H100 NVL GPU with 94 GB of memory, 40 AMD EPYC Genoa processor cores, and 320 GB of system memory. Architectural security features including AMD SEV-SNP [32] and NVIDIA GPU CC [34] are always enabled.

The software stack in the CVM includes Ubuntu 24.04 with kernel version 6.11.0-1018-azure, NVIDIA open driver version 570.158.01, CUDA 12.8, Python 3.12.3, and PyTorch 2.7.1. For LLM, our evaluation utilizes Llama 2 [26] with 7B and 13B, Llama 3 [65] with 8B, Llama 3.2 with 1B and 3B, and Code Llama [66] with 7B, 13B and 34B parameters.

For overhead evaluation, we measure the latency both with Nvidia MPS [67] enabled and disabled. It is worth noting that, to use MPS, it requires no modifications to our implementation.

### A. Empirical Security Measurements of Prompt Obfuscation

As proven in §V-B, the security of Prompt Obfuscation is quantified by the available pair of security factors  $(\epsilon, \lambda)$ . These factors respectively determine the indistinguishability of fake n-grams from the sensitive segment, and the number of fake n-grams. We examine the available  $(\epsilon, \lambda)$  pairs with respect to various categories of personally identifiable information (PII).

**Dataset Preparation** We first construct the clinical dataset by combining clinical dialogues between patients and physicians [68] with clinical notes from USMLE Step 2 [69]. Additionally, we use a public resume classification dataset from Kaggle [70]. To categorize and tag the PII data, we use Google’s PII detection tool, marking each instance with a tag. Details are provided in §E.

**Exhaustive Sampling** We present the results of the examined  $(\epsilon, \lambda)$  pairs for various PII categories in Figure 4 and Figure 5. We note that the x-axis is  $1/\epsilon$  instead of  $\epsilon$  for better visualization, and the higher  $\lambda$  the better. These pairs are determined via an exhaustive search using the GQS algorithm (Algorithm 1)

on both datasets, with Llama 3,  $\lambda_{\max} = 512$ , and sampling temperature  $\tau = 0$ .

**Result Analysis** The results indicate that GQS can generate a reasonably large set of fake n-grams. For example, with  $\epsilon = 0.1$ , the “date” category has approximately  $\lambda = 360$ , which roughly corresponds to the number of days in a year, and the “age” category has  $\lambda = 52$ , reflecting age groups from 18 to 70. Examples of dataset samples and GQS outputs are provided in §E.

**Effect of Different Models and Parameter Size** The impact of the model parameter size on  $\lambda$  is relatively small. For example, comparing Llama 2 models with 7B and 13B parameters on the clinical dataset results in only a 4% difference in  $\lambda$ . In contrast, the choice of language model has a more substantial effect on  $\lambda$ . In Figure 6, there is a  $2.4\times$  difference in  $\lambda$  between Llama 3 and Llama 2 (13B). We observed that Llama 3, as a more advanced model than Llama 2, is more “confident” in selecting the next token, which narrows the possible candidate pool. In other words, the distribution modeled by Llama 2 is flatter, resulting in a larger  $\lambda$  under the same conditions.

**Effect of Regularization** Grammar and typing errors in the sensitive segment degrade the security of Prompt Obfuscation, as sequences with such errors are far less common in the distribution. Regularizing the content, such as correcting capitalization and spelling, can improve  $\lambda$ . We use a ChatGPT-based tool to correct typing errors in the dataset and compare the  $\lambda$  between regularized (“Llama3+Reg”) and non-regularized (“Llama3”) datasets in Figure 6.

**Effect of Sampling Temperature** The token sampling temperature  $\tau$  also influences the  $\lambda$  values. A higher  $\tau$  flattens the token distribution, increasing the number of fake n-grams that fall within the same quantized bin as the authentic segment (Algorithm 1). We present the difference in  $\lambda$  between  $\tau = 1$  (“Llama3+Reg”) and  $\tau = 2$  in Figure 6.

### B. Performance Analysis

We compare our approach with two baselines: (1) *No protection*, a naive approach where a LLM instance serves all users within a single process (Figure 2b), which is not secure and intended to demonstrate the upper bound of performance; and (2) *Full isolation*, a naive approach where each user is assigned to a dedicated LLM instance within a per-user process (Figure 2c). Our approach is denoted as *SPD* (or *SPD+PO*) (Figure 2d). As mentioned in *Evaluation Setup*, we measure the latency with both Nvidia MPS [67] enabled and disabled.

**1) Scalability:** Our evaluation setup includes 1 to 32 users, with both prompts and responses ranging from 64 to 512 tokens. We measure the end-to-end latency for each user to receive the responses. Figure 7, Figure 8 and Figure 9 summarize the main results, demonstrating that our approach scales effectively as the number of users, input/output tokens, and the model parameter size increase.

**Number of Users** The *Full isolation* approach faces inherent scalability limitations due to GPU memory constraints as it

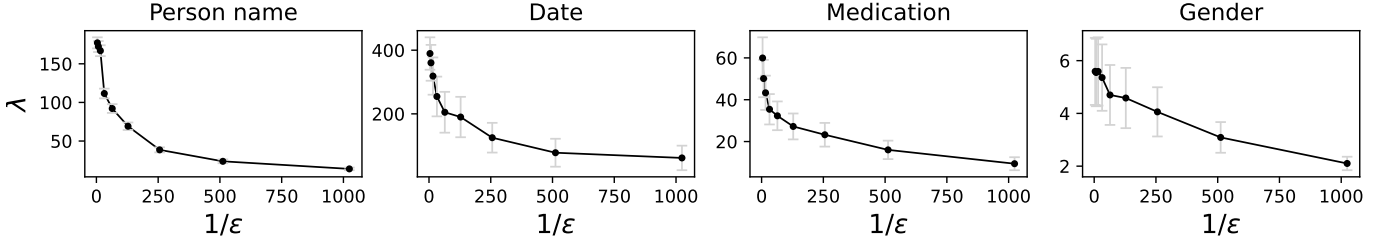


Fig. 4:  $(\epsilon, \lambda)$  pairs sampled from the clinical dataset with  $\lambda_{\max} = 512$ , for four selected PII categories (person name, date, medication and gender). Dots indicate the mean of  $\lambda$  for each  $\epsilon$ , and the error bars indicate a 95% interval.

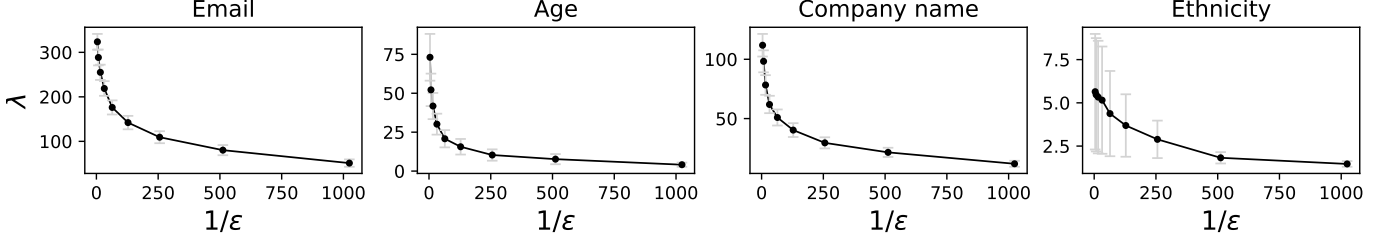


Fig. 5:  $(\epsilon, \lambda)$  pairs sampled from the resume dataset with  $\lambda_{\max} = 512$ , for four selected PII categories (email, age, company name and ethnicity). Dots indicate the mean of  $\lambda$  for each  $\epsilon$ , and the error bars indicate a 95% interval.

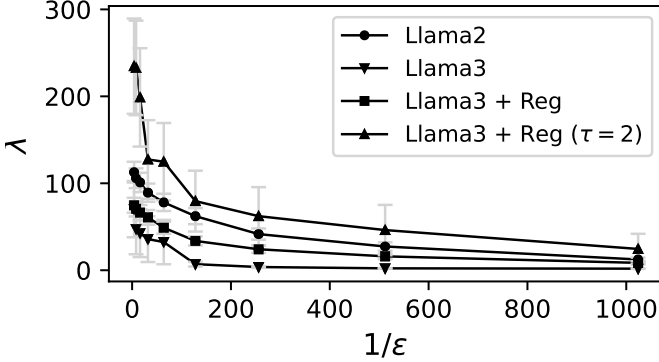


Fig. 6:  $(\epsilon, \lambda)$  pairs sampled from the clinical dataset with  $\lambda_{\max} = 512$ , for locational PII, e.g. name of places. Unless otherwise specified, the sampling temperature is set to  $\tau = 1$ .

provides separate LLM instances for each user. As shown in Figure 7, it exhibits significant latency degradation with increasing user counts. In contrast, OSPD achieves superior scalability, as it maintains a substantially smaller memory footprint. However, our approach still faces high overhead compared to the *No protection* approach (indicated as  $y = 1$ ), which is the cost of isolating user prompts in per-user processes.

**Model Parameter Size** Figure 8 shows the generation slows down for all approaches as the size of model parameter increases. Not surprisingly, *No protection* performs the best, while *SPD* is less affected by parameter size scaling compared to the *Full isolation* approach, as *Full isolation*’s end-to-end latency scales at a higher rate than that of *SPD* under the same conditions, when the model size increases from 1B to 34B.

**Number of Input/Output Tokens** Figure 9 shows both input and output token counts have negligible impact on token generation. As the counts increase, the latency per token

remains relatively stable as decoding each token has static overhead, or even slightly reduces because the initial cost is amortized across the tokens. In contrast, PO incurs non-trivial overhead to generation. We discuss it in the following sections.

2) *Compute efficiency*: We further breakdown the overhead of OSPD to demonstrate the sources of overhead.

**Overhead breakdown of SPD** *SPD* introduces overhead mainly due to (1) the absence of batch processing in per-user processes, and (2) communication between user processes and the LLM. We present *SPD*’s latency breakdown in Figure 10. The seven latency components align with the processing steps in Figure 3, except that we partition the “QKV projection” into “Q proj” and “KV proj”. The first bar in Figure 10 represents the breakdown of *No protection*, while other bars represent that of *SPD* in different conditions. The three bars in the middle differ in when  $Q$  is sent, right after the computation of  $Q$  (“After Q”),  $K$  and  $V$  (“After KV”), or the public attention scores (“After Pub”). The last bar is measured with GPU CC disabled. We note Figure 10 is measured with CUDA Event, which is slightly different from the end-to-end latency in previous measurements.

**Processes compete for GPU resources** By comparing the first four bars, we observe that the computation right after sending  $Q$  is much slowed down compared to the *No protection* baseline, while other components have negligible overhead. It is because the user processes compete with the LLM for GPU resources once they receive  $Q$ . Sending  $Q$  after public attention computation can avoid such competition, but the LLM must wait for the private scores, which leads to slightly higher total latency as it fails to overlap communication with computation.

**High communication overhead of GPU CC** The last bar in Figure 10 shows *SPD*’s latency breakdown with GPU CC disabled. Its total latency is 1/3 of that with GPU CC enabled as the communication overhead reduces by about  $5\times$ . This is

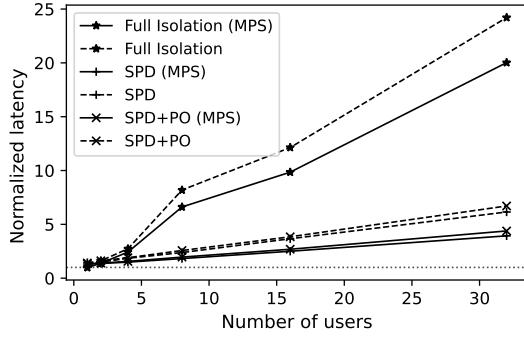


Fig. 7: **Normalized latency with varying number of users**, Llama 3 (8B), 64 input and 64 output tokens,  $\lambda = 7$  for PO.  $y = 1$  indicates the latency of No Protection baseline.

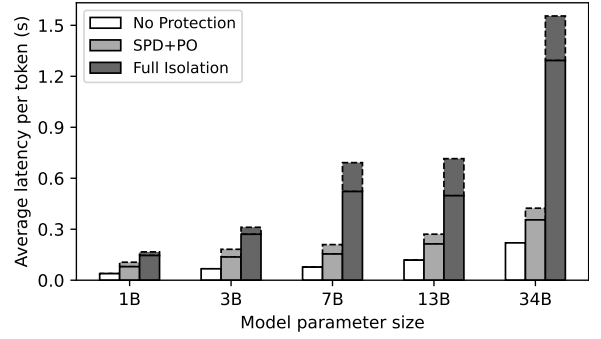


Fig. 8: **Average latency with varying model sizes**, 8 users, 64 input and 64 output tokens,  $\lambda = 7$  for PO. The solid and dashed bars indicate with and without MPS respectively.

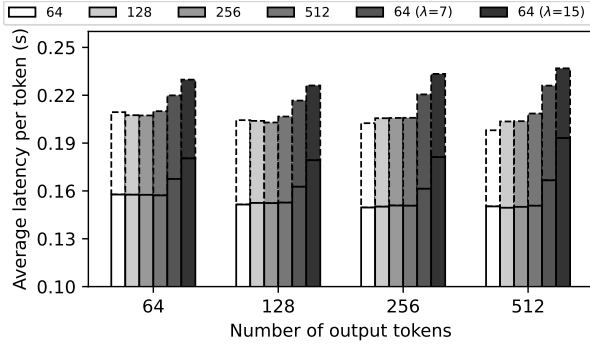


Fig. 9: **Average latency per generated token, with varying number of input, output tokens and  $\lambda$** , Llama 3 (8B) and 8 users. Varying groups of bars indicate varying output token counts. The first four bars in each group indicate varying input token counts while  $\lambda = 0$ . The last two bars in each group indicate different  $\lambda$  with 64 input tokens. The solid and dashed bars indicate with and without MPS respectively.

because the GLOO backend [62] transfers tensors via the host, where the GPU CC encrypts and decrypts all transferred data, incurring high overhead [71]. We expect this overhead can be much reduced and even fully eliminated with newer version GPU CC designs [72] or better support of communication between processes that share the same GPU (See §VIII-B).

**Overhead of PO** PO introduces overhead due to (1) sampling fake n-grams for virtual prompts, which increases time-to-first-token (TTFT) latency, and (2) decoding for  $\lambda$  virtual prompts. For (1), Figure 11 illustrates the sampling latency for virtual prompts. The average sampling time for an eight-token replacement using  $\lambda = 512$  and  $\epsilon = 1/32$  is around 1 second. Sampling multiple subsequences can be batched, for example, 16 subsequences take about 1.5 seconds. Lower  $\epsilon$  results in faster sampling due to a reduced  $\lambda$ . For (2), the impact of decoding virtual prompts is reflected in Figure 9. With eight users, the overhead is about 8% on average when  $\lambda = 7$ , while 15 to 20% when  $\lambda = 15$ . It indicates the overhead is relatively small when  $\lambda$  is small, because the GPU is typically underutilized due to the lack of batch parallelism in a user

process. However, such overhead increases more rapidly when  $\lambda$  grows larger, where computation from multiple user processes may become the bottleneck and keep the LLM process waiting.

## VIII. DISCUSSION

In this section, we first discuss attacks out of our threat model and how OSPD collaborates with existing solutions to mitigate them. Then, we discuss the portability of OSPD design and how to deploy it under different situations. Finally, we discuss the limitations of OSPD and its future work.

### A. Mitigating Attacks Out of Scope

**Prompt-leakage Injection Attacks** A malicious LLM may cause the user process to leak prompts by injecting instructions like “repeat the prompt” into the inference process via manipulating the token generation. Although this attack is outside our Honest-but-Curious (HBC) threat model, OSPD can work with attention-based detection methods to defend against it. Recently, researchers have discovered the *distraction effect* in attention computation when injected instructions are present. Building on this discovery, Attention Tracker effectively detects prompt injection attacks by tracking attention patterns [73].

**Attacks on TCB** OSPD introduces a novel approach to confidential prompting at application level, whose security is built on top of the trusted CVM hardware and software stack like its guest OS. That is, OSPD does not defend against attacks that compromise the CVM [74], [75] or its guest OS [76], [77]. However, as OSPD’s design is general, it is orthogonal to and compatible with any solution that enhances the security of CVM [78], [79] and its guest OS [36], [37], [80].

### B. Portability and Deployment of OSPD

**Portability across LLMs** We design OSPD to be portable across different decoder-only LLMs such as GPT [25] and Llama [26] series. But it does not work for encoder models as its design leverages the KV cache mechanism. Although our prototype and evaluation focus on the Llama series, we believe OSPD is applicable to other decoder-only LLMs, e.g., the GPT series. This is because our attention decomposition (Theorem 1) is general without relying on specific implementations.

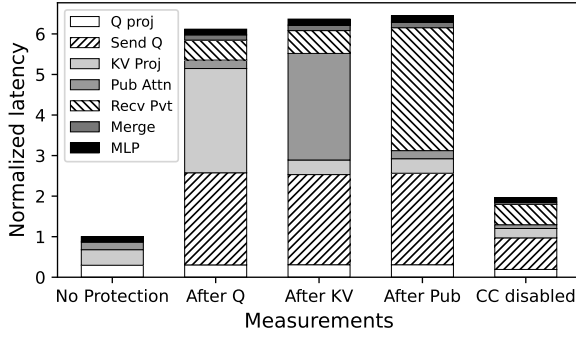


Fig. 10: **Overhead breakdown.** All are measured with Llama 3 (8B), 32 users, 64 input and 64 output tokens, and  $\lambda = 0$ . MPS is enabled except for *No Protection*.

**Portability across Architectures** We design OSPD to be portable across different CPU and GPU architectures, provided they support a CVM spanning both CPU and GPU. We deploy our prototype in an Azure CVM with an NVIDIA H100 GPU because it is the only CVM available on public cloud that enables GPU CC [34]. We believe OSPD can also be deployed in other CVMs with various architectures, in combinations such as Intel TDX [33] or ARM CCA [81] with NVIDIA Blackwell [72] or other GPU TEE solutions [82], [83], [84].

**Portability across Communication Backends** We use GLOO [62] as it is general. In contrast, even NCCL [63] typically performs better in scenarios involves GPUs, it requires each process has exclusive access to a GPU, which is not suitable for our evaluation platform, the only CVM available on public cloud enabling GPU CC. CUDA IPC and PyTorch’s Queue and Pipe can share tensors across processes without copying. However, so far they do not support asynchronous IO. As a result, they are even less efficient. Fortunately, we can expect the newer version of GPU CC in Nvidia Blackwell [72] with TEE-IO can reduce and even eliminate the overhead of encrypted communication between CPU and GPU. Any CUDA IPC based asynchronous IO support will also benefit OSPD.

**Per-user CVM Deployment without Consensus** In §III-B, we assume all users and the LLM provider trust the shared software stack. This consensus may not be practical when considering the OS has a large attack surface. OSPD is portable to per-user CVM instead of per-user process deployment. This deployment does not require the consensus on software stack, as each user can independently trust their own stack. However, to secure model confidentiality, this setup requires the cloud provider to inspect outbound data from user CVMs. This means the LLM provider must trust the cloud provider, or both being the same party, e.g., Google Gemini and Google Cloud.

**Achieve Consensus with A Smart Contract** It is interesting to view the initialization of OSPD (§III-C) from a decentralized perspective. We do not care which party initializes the CVM, as long as all parties agree on its initial state. We can standardize the properties and initialization of the CVM with a smart contract, hardcoding the target cloud platform, versions of the

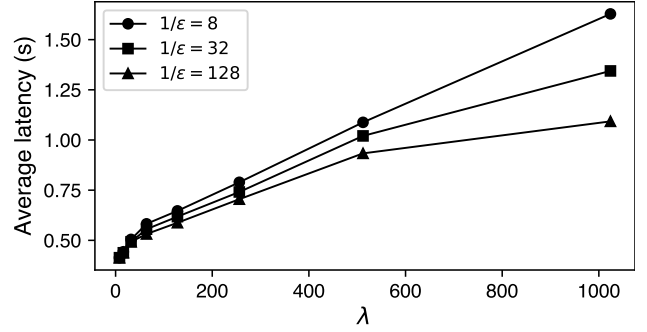


Fig. 11: Average latency of sampling virtual prompts with varying  $\lambda_{\max}$  and  $\epsilon$  for eight-token replacement in Llama 3.

software stack, minimum number of participants that triggers the initialization and so on. This smart contract can be certified by an authoritative auditor like CertiK [85], which eases the process of earning trust from users and the LLM provider.

**The More Trust, The Better Performance** In §III-B, we assume all users untrust each other and assign each user a dedicated process. In practice, some users may trust each other to some extent, e.g., a group of employees in a company. In this case, OSPD can assign a process shared by multiple users, reducing overhead of process management and switching.

### C. Limitations and future work

OSPD has several limitations, which bring new opportunities for future works. We hope our design and the following discussion will spark further exploration on confidential prompting.

**Redundant LLM Weights Loading** During prefill, each user process loads LLM weights independently, which is redundant and inefficient. To optimize, we can share weights residing in GPU memory across processes via CUDA IPC, which is supported by both CUDA and PyTorch APIs. However, we did not employ this optimization because CUDA does not support read-only sharing. A malicious user process may alter the shared weights to attack other users. This inspires us to consider a more secure way to share LLM weights, which likely requires lower-level development such as CUDA modification.

**Protection of LLM Response** OSPD secures user prompts but not the responses. This implies that the full isolation approach (Figure 2c) is still needed when user would like to secure both the prompts and responses against an untrusted LLM provider. OSPD offers an alternative approach for different scenarios instead of replacing existing confidential inferencing solutions.

## IX. CONCLUDING REMARKS

Cloud-hosted LLM serving is becoming pervasive in our daily lives but raises privacy concerns since users must submit their prompts to the cloud. OSPD combines two techniques to protect user prompts from LLM providers: secure partitioned decoding (SPD) and prompt obfuscation (PO). SPD fully leverages the confidential computing capabilities of modern hardware for efficient and scalable confidential prompting. PO, on the



other hand, leverages the statistical properties of advanced language model to achieve confidentiality without encryption. Our proposed techniques have the potential to enable privacy-preserving LLM applications such as chatbots and AI assistants that involve sensitive data such as personal information, clinical records, and financial documents.

## REFERENCES

- [1] P. Farrell, “JPMorgan restricts ChatGPT usage for its 250K staff over fears it could steal sensitive banking secrets,” <https://www.dailymail.co.uk/news/article-11780501/JPMorgan-restricts-ChatGPT-usage-250-000-staff-data-privacy-fears.html>, 2023.
- [2] S. Ray, “Apple Joins A Growing List Of Companies Cracking Down On Use Of ChatGPT By Staffers—Here’s Why,” <https://www.forbes.com/sites/siladityaray/2023/05/19/apple-joins-a-growing-list-of-companies-cracking-down-on-use-of-chatgpt-by-staffers-heres-why/?sh=49380e9628ff>, 2023.
- [3] EU, “General Data Protection Regulation (GDPR),” <https://gdpr-info.eu/>, 2016.
- [4] U. HHS, “Health Insurance Portability and Accountability Act of 1996 (HIPAA),” <https://www.cdc.gov/php/php/resources/health-insurance-portability-and-accountability-act-of-1996-hipaa.html>, 1996.
- [5] N. Lomas, “Italy orders ChatGPT blocked citing data protection concerns,” <https://techcrunch.com/2023/03/31/chatgpt-blocked-italy/>, 2023.
- [6] J. Lin, J. Tang, H. Tang, S. Yang, W.-M. Chen, W.-C. Wang, G. Xiao, X. Dang, C. Gan, and S. Han, “AWQ: Activation-aware weight quantization for LLM compression and acceleration,” in *MLSys*, 2024.
- [7] T. Wu, A. Panda, J. T. Wang, and P. Mittal, “Privacy-preserving in-context learning for large language models,” *arXiv preprint arXiv:2305.01639*, 2023.
- [8] X. Tang, R. Shin, H. A. Inan, A. Manoel, F. Mirehshghallah, Z. Lin, S. Gopi, J. Kulkarni, and R. Sim, “Privacy-preserving in-context learning with differentially private few-shot generation,” *arXiv preprint arXiv:2309.11765*, 2023.
- [9] Z. Shen, Z. Xi, Y. He, W. Tong, J. Hua, and S. Zhong, “The fire thief is also the keeper: Balancing usability and privacy in prompts,” *arXiv preprint arXiv:2406.14318*, 2024.
- [10] Z. Zeng, J. Wang, J. Yang, Z. Lu, H. Zhuang, and C. Chen, “PrivacyRestore: Privacy-preserving inference in large language models via privacy removal and restoration,” *arXiv preprint arXiv:2406.01394*, 2024.
- [11] Y. Chen, T. Li, H. Liu, and Y. Yu, “Hide and Seek (HaS): A lightweight framework for prompt privacy protection,” *arXiv preprint arXiv:2309.03057*, 2023.
- [12] Z. Kan, L. Qiao, H. Yu, L. Peng, Y. Gao, and D. Li, “Protecting user privacy in remote conversational systems: A privacy-preserving framework based on text sanitization,” *arXiv preprint arXiv:2306.08223*, 2023.
- [13] Z. Huang, W.-j. Lu, C. Hong, and J. Ding, “Cheetah: Lean and fast secure two-party deep neural network inference,” in *31st USENIX Security Symposium (USENIX Security 22)*, 2022, pp. 809–826.
- [14] M. Hao, H. Li, H. Chen, P. Xing, G. Xu, and T. Zhang, “Iron: Private inference on transformers,” *Advances in neural information processing systems*, vol. 35, pp. 15 718–15 731, 2022.
- [15] C. C. C. (CCC), “The Linux Foundation Projects,” <https://confidentialcomputing.io/>, 2023.
- [16] T. Lee, Z. Lin, S. Pushp, C. Li, Y. Liu, Y. Lee, F. Xu, C. Xu, L. Zhang, and J. Song, “Occlumency: Privacy-preserving remote deep-learning inference using SGX,” in *The 25th Annual International Conference on Mobile Computing and Networking*, 2019, pp. 1–17.
- [17] M. Russinovich, “Azure AI Confidential Inferencing: Technical Deep-Dive,” <https://techcommunity.microsoft.com/t5/azure-confidential-computing/azure-ai-confidential-inferencing-technical-deep-dive/ba-p/4253150>, 2024.
- [18] C. Renzo, L. Aliberti, J. Miles, and J. Kovba, “Large language model inference over confidential data using AWS Nitro Enclaves,” <https://aws.amazon.com/blogs/machine-learning/large-language-model-inference-over-confidential-data-using-aws-nitro-enclaves/>, 2024.
- [19] Y. Tan, X. Shen, Y. Shen, M. Backes, and Y. Zhang, “On the effectiveness of prompt stealing attacks on in-the-wild prompts,” in *2025 IEEE Symposium on Security and Privacy (SP)*. IEEE, 2025, pp. 392–410.
- [20] L. Gao, R. Peng, Y. Zhang, and J. Zhao, “Dory: Deliberative prompt recovery for LLM,” *arXiv preprint arXiv:2405.20657*, 2024.
- [21] Z. Sha and Y. Zhang, “Prompt stealing attacks against large language models,” *arXiv preprint arXiv:2402.12959*, 2024.
- [22] Y. Yang, X. Zhang, Y. Jiang, X. Chen, H. Wang, S. Ji, and Z. Wang, “Prsa: Prompt reverse stealing attacks against large language models,” *CoRR*, 2024.
- [23] A. Radford, J. Wu, R. Child, D. Luan, D. Amodei, I. Sutskever *et al.*, “Language models are unsupervised multitask learners,” *OpenAI blog*, vol. 1, no. 8, p. 9, 2019.
- [24] T. Brown, B. Mann, N. Ryder, M. Subbiah, J. D. Kaplan, P. Dhariwal, A. Neelakantan, P. Shyam, G. Sastry, A. Askell *et al.*, “Language models are few-shot learners,” *Advances in neural information processing systems*, vol. 33, pp. 1877–1901, 2020.
- [25] J. Achiam, S. Adler, S. Agarwal, L. Ahmad, I. Akkaya, F. L. Aleman, D. Almeida, J. Altenschmidt, S. Altman, S. Anadkat *et al.*, “GPT-4 technical report,” *arXiv preprint arXiv:2303.08774*, 2023.
- [26] H. Touvron, T. Lavril, G. Izacard, X. Martinet, M.-A. Lachaux, T. Lacroix, B. Rozière, N. Goyal, E. Hambro, F. Azhar *et al.*, “LLaMA: Open and efficient foundation language models,” *arXiv preprint arXiv:2302.13971*, 2023.
- [27] A. Vaswani, N. Shazeer, N. Parmar, J. Uszkoreit, L. Jones, A. N. Gomez, Ł. Kaiser, and I. Polosukhin, “Attention is all you need,” *Advances in neural information processing systems*, vol. 30, 2017.
- [28] M. Ott, S. Edunov, A. Baevski, A. Fan, S. Gross, N. Ng, D. Grangier, and M. Auli, “fairseq: A fast, extensible toolkit for sequence modeling,” in *Proceedings of the 2019 Conference of the North American Chapter of the Association for Computational Linguistics: Human Language Technologies, NAACL-HLT 2019, Minneapolis, MN, USA, June 2-7, 2019, Demonstrations*, W. Ammar, A. Louis, and N. Mostafazadeh, Eds. Association for Computational Linguistics, 2019, pp. 48–53. [Online]. Available: <https://doi.org/10.18653/v1/n19-4009>
- [29] M. Shoenybi, M. Patwary, R. Puri, P. LeGresley, J. Casper, and B. Catanzaro, “Megatron-LM: Training multi-billion parameter language models using model parallelism,” *CoRR*, vol. abs/1909.08053, 2019. [Online]. Available: <http://arxiv.org/abs/1909.08053>
- [30] R. Pope, S. Douglas, A. Chowdhery, J. Devlin, J. Bradbury, J. Heek, K. Xiao, S. Agrawal, and J. Dean, “Efficiently scaling transformer inference,” *Proceedings of Machine Learning and Systems*, vol. 5, pp. 606–624, 2023.
- [31] I. Gim, G. Chen, S.-s. Lee, N. Sarda, A. Khandelwal, and L. Zhong, “Prompt Cache: Modular attention reuse for low-latency inference,” *arXiv preprint arXiv:2311.04934*, 2023.
- [32] AMD, “AMD secure encrypted virtualization (SEV),” <https://www.amd.com/en/developer/sev.html>, 2023.
- [33] Intel, “Intel trust domain extensions (Intel TDX),” <https://www.intel.com/content/www/us/en/developer/articles/technical/intel-trust-domain-extensions.html>, 2023.
- [34] Nvidia, “NVIDIA Confidential Computing,” <https://www.nvidia.com/en-us/data-center/solutions/confidential-computing/>, 2023.
- [35] G. Wu, Z. Zhang, Y. Zhang, W. Wang, J. Niu, Y. Wu, and Y. Zhang, “I know what you asked: Prompt leakage via kv-cache sharing in multi-tenant llm serving,” in *Proceedings of the 2025 Network and Distributed System Security (NDSS) Symposium. San Diego, CA, USA, 2025*.
- [36] S. Zhao, M. Li, Y. Zhang, and Z. Lin, “vSGX: Virtualizing SGX enclaves on AMD SEV,” in *2022 IEEE Symposium on Security and Privacy (SP)*. IEEE, 2022, pp. 321–336.
- [37] W. Wang, L. Song, B. Mei, S. Liu, S. Zhao, S. Yan, X. Wang, D. Meng, and R. Hou, “The road to trust: Building enclaves within confidential VMs,” *arXiv preprint arXiv:2402.11438*, 2024.
- [38] C. E. Shannon, “Communication theory of secrecy systems,” *The Bell system technical journal*, vol. 28, no. 4, pp. 656–715, 1949.
- [39] U. Maurer, “Information-theoretic cryptography,” in *Advances in Cryptology — CRYPTO ’99*, ser. Lecture Notes in Computer Science, M. Wiener, Ed., vol. 1666. Springer-Verlag, 8 1999, pp. 47–64.
- [40] R. L. Rivest, “Chaffing and winnowing: Confidentiality without encryption,” *CryptoBytes (RSA laboratories)*, vol. 4, no. 1, pp. 12–17, 1998.
- [41] M. Bellare and A. Boldyreva, “The security of chaffing and winnowing,” in *Advances in Cryptology—ASIACRYPT 2000: 6th International Conference on the Theory and Application of Cryptology and Information Security Kyoto, Japan, December 3–7, 2000 Proceedings 6*. Springer, 2000, pp. 517–530.
- [42] W. Kwon, Z. Li, S. Zhuang, Y. Sheng, L. Zheng, C. H. Yu, J. Gonzalez, H. Zhang, and I. Stoica, “Efficient memory management for large language model serving with PagedAttention,” in *Proceedings of the 29th symposium on operating systems principles*, 2023, pp. 611–626.
- [43] L. Zheng, L. Yin, Z. Xie, J. Huang, C. Sun, C. Yu, S. Cao, C. Kozyrakis, I. Stoica, J. E. Gonzalez *et al.*, “Efficiently programming large language models using SGLang,” 2023.
- [44] K. Edemacu and X. Wu, “Privacy preserving prompt engineering: A survey,” *arXiv preprint arXiv:2404.06001*, 2024.
- [45] A. Panda, T. Wu, J. T. Wang, and P. Mittal, “Differentially private in-context learning,” *arXiv preprint arXiv:2305.01639*, 2023.

- [46] J. Hong, J. T. Wang, C. Zhang, Z. Li, B. Li, and Z. Wang, "DP-OPT: Make large language model your privacy-preserving prompt engineer," 2024.
- [47] Y. Akimoto, K. Fukuchi, Y. Akimoto, and J. Sakuma, "Privformer: Privacy-preserving transformer with MPC," in *2023 IEEE 8th European Symposium on Security and Privacy (EuroS&P)*. IEEE, 2023, pp. 392–410.
- [48] D. Li, R. Shao, H. Wang, H. Guo, E. P. Xing, and H. Zhang, "MPCFormer: fast, performant and private transformer inference with MPC," *arXiv preprint arXiv:2211.01452*, 2022.
- [49] X. Liu and Z. Liu, "LLMs can understand encrypted prompt: Towards privacy-computing friendly transformers," *arXiv preprint arXiv:2305.18396*, 2023.
- [50] Q. Pang, J. Zhu, H. Möllering, W. Zheng, and T. Schneider, "BOLT: Privacy-preserving, accurate and efficient inference for transformers," in *2024 IEEE Symposium on Security and Privacy (SP)*. IEEE, 2024, pp. 4753–4771.
- [51] T. Chen, H. Bao, S. Huang, L. Dong, B. Jiao, D. Jiang, H. Zhou, J. Li, and F. Wei, "THE-X: Privacy-preserving transformer inference with homomorphic encryption," *arXiv preprint arXiv:2206.00216*, 2022.
- [52] Y. Yao, F. Wang, S. Ravi, and M. Chen, "Privacy-preserving language model inference with instance obfuscation," *arXiv preprint arXiv:2402.08227*, 2024.
- [53] P. Mai, Y. Yang, R. Yan, R. Ye, and Y. Pang, "ConfusionPrompt: Practical private inference for online large language models," *Available at SSRN 5046754*, 2023.
- [54] M. Zhang, T. He, T. Wang, L. Mi, N. Mireshghallah, B. Chen, H. Wang, and Y. Tsvetkov, "LatticeGen: Hiding generated text in a lattice for privacy-aware large language model generation on cloud," in *Findings of the Association for Computational Linguistics: NAACL 2024*, 2024, pp. 2674–2690.
- [55] M. Milakov and N. Gimelshein, "Online normalizer calculation for softmax," *arXiv preprint arXiv:1805.02867*, 2018.
- [56] J. Devlin, M.-W. Chang, K. Lee, and K. Toutanova, "BERT: Pre-training of deep bidirectional transformers for language understanding," *arXiv preprint arXiv:1810.04805*, 2018.
- [57] C. Donahue, M. Lee, and P. Liang, "Enabling language models to fill in the blanks," *arXiv preprint arXiv:2005.05339*, 2020.
- [58] M. Bavarian, H. Jun, N. Tezak, J. Schulman, C. McLeavey, J. Tworek, and M. Chen, "Efficient training of language models to fill in the middle," *arXiv preprint arXiv:2207.14255*, 2022.
- [59] X. Ning, Z. Lin, Z. Zhou, H. Yang, and Y. Wang, "Skeleton-of-Thought: Large language models can do parallel decoding," *arXiv preprint arXiv:2307.15337*, 2023.
- [60] R. Li, L. B. Allal, Y. Zi, N. Muennighoff, D. Kocetkov, C. Mou, M. Marone, C. Akiki, J. Li, J. Chim *et al.*, "StarCoder: may the source be with you!" *arXiv preprint arXiv:2305.06161*, 2023.
- [61] T. Wolf, L. Debut, V. Sanh, J. Chaumond, C. Delangue, A. Moi, P. Cistac, T. Rault, R. Louf, M. Funtowicz, J. Davison, S. Shleifer, P. von Platen, C. Ma, Y. Jernite, J. Plu, C. Xu, T. L. Scao, S. Gugger, M. Drame, Q. Lhoest, and A. M. Rush, "Transformers: State-of-the-art natural language processing," in *Proceedings of the 2020 Conference on Empirical Methods in Natural Language Processing: System Demonstrations*. Online: Association for Computational Linguistics, Oct. 2020, pp. 38–45. [Online]. Available: <https://www.aclweb.org/anthology/2020.emnlp-demos.6>
- [62] Facebook, "Gloo: Collective Communications Library," 2023, accessed: 2024-11-09. [Online]. Available: <https://github.com/facebookincubator/gloo>
- [63] Nvidia, "NVIDIA Collective Communications Library (NCCL)," 2025, accessed: 2025-08-07. [Online]. Available: <https://developer.nvidia.com/nccl>
- [64] Microsoft, "Microsoft Azure NCCads\_H100\_v5 sizes series," <https://learn.microsoft.com/en-us/azure/virtual-machines/sizes/gpu-accelerated/nccadsh100v5-series>, 2024.
- [65] Meta, "Llama 3," <https://llama.meta.com/llama3/>, 2024.
- [66] "Code Llama," <https://ai.meta.com/blog/code-llama-large-language-model-coding/>, 2024.
- [67] Nvidia, "NVIDIA MPS," <https://docs.nvidia.com/deploy/mps/index.html>, 2025.
- [68] A. Ben Abacha, W.-w. Yim, Y. Fan, and T. Lin, "An empirical study of clinical note generation from doctor-patient encounters," in *Proceedings of the 17th Conference of the European Chapter of the Association for Computational Linguistics*. Dubrovnik, Croatia: Association for Computational Linguistics, May 2023, pp. 2291–2302. [Online]. Available: <https://aclanthology.org/2023.eacl-main.168>
- [69] NBME, "Score clinical patient notes," *Kaggle competition*, 2022. [Online]. Available: <https://www.kaggle.com/competitions/nbme-score-clinical-patient-notes>
- [70] A. Mitsu and T. Yoshihide, "Resume text classification dataset," *Kaggle competition*, 2021. [Online]. Available: <https://www.kaggle.com/datasets/chingkuangkam/resume-text-classification-dataset>
- [71] Nvidia, "NVIDIA Confidential Computing Whitepaper," <https://images.nvidia.com/aem-dam/en-zz/Solutions/data-center/HCC-Whitepaper-v1.0.pdf>, 2023.
- [72] —, "NVIDIA Blackwell Architecture," <https://www.nvidia.com/en-us/data-center/technologies/blackwell-architecture/>, 2025.
- [73] K.-H. Hung, C.-Y. Ko, A. Rawat, I. Chung, W. H. Hsu, P.-Y. Chen *et al.*, "Attention Tracker: Detecting prompt injection attacks in LLMs," *arXiv preprint arXiv:2411.00348*, 2024.
- [74] M. Li, Y. Zhang, H. Wang, K. Li, and Y. Cheng, "CIPHERLEAKS: Breaking constant-time cryptography on AMD SEV via the ciphertext side channel," in *30th USENIX Security Symposium (USENIX Security 21)*, 2021, pp. 717–732.
- [75] Y. Yuan, Z. Liu, S. Deng, Y. Chen, S. Wang, Y. Zhang, and Z. Su, "CipherSteal: Stealing input data from TEE-shielded neural networks with ciphertext side channels," in *2025 IEEE Symposium on Security and Privacy (SP)*. IEEE, 2025, pp. 4136–4154.
- [76] B. Schlüter, S. Sridhara, A. Bertschi, and S. Shinde, "WeSee: Using malicious #VC interrupts to break AMD SEV-SNP," in *2024 IEEE Symposium on Security and Privacy (SP)*. IEEE, 2024, pp. 4220–4238.
- [77] B. Schlüter, S. Sridhara, M. Kuhne, A. Bertschi, and S. Shinde, "HECKLER: Breaking confidential VMs with malicious interrupts," in *33rd USENIX Security Symposium (USENIX Security 24)*, 2024, pp. 3459–3476.
- [78] K. D. Duy, J. Kim, H. Lim, and H. Lee, "INCOGNITOS: A practical unikernel design for full-system obfuscation in confidential virtual machines," in *2025 IEEE Symposium on Security and Privacy (SP)*. IEEE, 2025, pp. 4192–4209.
- [79] H. Qin, Z. Song, W. Zhang, S. Huang, W. Yao, G. Liu, X. Jia, and H. Du, "Protecting encrypted virtual machines from nested page fault controlled channel," in *Proceedings of the Thirteenth ACM Conference on Data and Application Security and Privacy*, 2023, pp. 165–175.
- [80] C. Li, S.-s. Lee, and L. Zhong, "Blindfold: Confidential memory management by untrusted operating system," *arXiv preprint arXiv:2412.01059*, 2024.
- [81] ARM, "Introducing Arm Confidential Compute Architecture," <https://developer.arm.com/documentation/den0125/400>, 2025.
- [82] S. Volos, K. Vaswani, and R. Bruno, "Graviton: Trusted execution environments on GPUs," in *13th USENIX Symposium on Operating Systems Design and Implementation (OSDI 18)*, 2018, pp. 681–696.
- [83] C. Wang, F. Zhang, Y. Deng, K. Leach, J. Cao, Z. Ning, S. Yan, and Z. He, "CAGE: Complementing Arm CCA with GPU extensions," in *Network and Distributed System Security (NDSS) Symposium*, vol. 2024, 2024.
- [84] S. Sridhara, A. Bertschi, B. Schlüter, M. Kuhne, F. Aliberti, and S. Shinde, "ACAI: Protecting accelerator execution with Arm confidential computing architecture," in *33rd USENIX Security Symposium (USENIX Security 24)*, 2024, pp. 3423–3440.
- [85] CertiK, "Smart Contract Audit," 2025. [Online]. Available: <https://www.certi.k.com/products/smart-contract-audit>

## APPENDIX

### A. Proof of Theorem 1

Let  $Q \in \mathbb{R}^d$  be the query vector. Partition the key and value matrices  $K, V \in \mathbb{R}^{n \times d}$  into private and public components:

$$K = \begin{bmatrix} K_{\text{Pvt}} \\ K_{\text{Pub}} \end{bmatrix}, \quad V = \begin{bmatrix} V_{\text{Pvt}} \\ V_{\text{Pub}} \end{bmatrix}.$$

Compute the attention scores  $s$  by:

$$s = QK^\top = [QK_{\text{Pvt}}^\top \quad QK_{\text{Pub}}^\top] = [s_{\text{Pvt}} \quad s_{\text{Pub}}],$$

where  $s_{\text{Pvt}} = QK_{\text{Pvt}}^\top$  and  $s_{\text{Pub}} = QK_{\text{Pub}}^\top$ . Define the softmax denominators:

$$\gamma = \sum_{i=1}^n \exp(s_i) = \gamma_{\text{Pvt}} + \gamma_{\text{Pub}},$$

with

$$\gamma_{\text{Pvt}} = \sum_{i=1}^{n_{\text{Pvt}}} \exp(s_{\text{Pvt},i}), \quad \gamma_{\text{Pub}} = \sum_{i=1}^{n_{\text{Pub}}} \exp(s_{\text{Pub},i}).$$

The attention output is:

$$\begin{aligned} \sigma(s)V &= \sum_{i=1}^n \frac{\exp(s_i)}{\gamma} V_i \\ &= \frac{1}{\gamma} \left( \sum_{i=1}^{n_{\text{Pvt}}} \exp(s_{\text{Pvt},i}) V_{\text{Pvt},i} + \sum_{i=1}^{n_{\text{Pub}}} \exp(s_{\text{Pub},i}) V_{\text{Pub},i} \right) \\ &= \frac{\gamma_{\text{Pvt}}}{\gamma} \left( \frac{1}{\gamma_{\text{Pvt}}} \sum_{i=1}^{n_{\text{Pvt}}} \exp(s_{\text{Pvt},i}) V_{\text{Pvt},i} \right) \\ &\quad + \frac{\gamma_{\text{Pub}}}{\gamma} \left( \frac{1}{\gamma_{\text{Pub}}} \sum_{i=1}^{n_{\text{Pub}}} \exp(s_{\text{Pub},i}) V_{\text{Pub},i} \right) \\ &= \frac{\gamma_{\text{Pvt}}}{\gamma} (\sigma(s_{\text{Pvt}})^\top V_{\text{Pvt}}) + \frac{\gamma_{\text{Pub}}}{\gamma} (\sigma(s_{\text{Pub}})^\top V_{\text{Pub}}). \end{aligned} \tag{8}$$

Thus,

$$\begin{aligned} \sigma(QK^\top)V &= \frac{\gamma_{\text{Pvt}}}{\gamma_{\text{Pvt}} + \gamma_{\text{Pub}}} \sigma(QK_{\text{Pvt}}^\top)V_{\text{Pvt}} \\ &\quad + \frac{\gamma_{\text{Pub}}}{\gamma_{\text{Pvt}} + \gamma_{\text{Pub}}} \sigma(QK_{\text{Pub}}^\top)V_{\text{Pub}}, \end{aligned} \tag{9}$$

which completes the proof.

### B. Proof of Equation 4

In the following proof, we assume that there is only one tagged segment  $S_{\text{tag}}$  in a user prompt  $S_0$  for simplicity. As discussed in §V-A, for cases where more than one sensitive segments are tagged, fake n-grams are sampled for each tagged segment in parallel, resulting in  $\epsilon_j = \epsilon/k$  for the  $j$ -th segment, where  $k$  is the number of sensitive segments and  $j = 1, \dots, k$ .

**Part I: Reducing Equation 4 to Equation 1** To begin with, for the  $i$ -th virtual prompt, where  $i = 1, \dots, \lambda$ , we have

$$\frac{LM(S_i)}{LM(S_0)} = \frac{LM(S_{\text{fake}_i} | S_0/S_{\text{tag}}) \cdot LM(S_0/S_{\text{tag}})}{LM(S_{\text{tag}} | S_0/S_{\text{tag}}) \cdot LM(S_0/S_{\text{tag}})},$$

where  $S_a/S_b$  denotes replacing segment  $S_b$  with empty slots in  $S_a$ . As a result, proving Equation 4 is equivalent to prove

$$\| \ln(LM(S_{\text{fake}_i} | S_0/S_{\text{tag}})) - \ln(LM(S_{\text{tag}} | S_0/S_{\text{tag}})) \| \leq \epsilon,$$

which is exactly Equation 1.

**Part II: Proof of Equation 1** Let's denote each token in  $S_{\text{tag}}$  as random variables  $X_1, \dots, X_n$ , where  $n$  is the number of tokens and  $X_i$  is the  $i$ -th token in  $S_{\text{tag}}$ . Let  $f(X_i) = LM(X_i | S_0/S_{\text{tag}}, X_1, \dots, X_{i-1})$  be the conditional probability of token  $X_i$ , as estimated by the language model  $LM$ , given the context  $S_0/S_{\text{tag}}$  and the previous tokens. Similarly, we represent the tokens in a fake sequence sampled by GQS as  $Y_1, \dots, Y_n$ , and let  $f(Y_i) = LM(Y_i | S_0/S_{\text{tag}}, Y_1, \dots, Y_{i-1})$ .

GQS partitions the next token distribution into  $\lceil \frac{1}{\epsilon'} \rceil$  bins, where  $\epsilon' = \epsilon/n$  and each bin contains tokens with probabilities falling in  $[e^{j\epsilon'}, e^{(j+1)\epsilon'})$ , where  $j$  is the bin index. Since GQS samples  $Y_i$  from the same bin as  $X_i$ , it is true for all  $i$  that

$$\| \ln(f(Y_i)) - \ln(f(X_i)) \| < \epsilon'.$$

As a result,

$$\begin{aligned} &\| \ln(LM(S_{\text{fake}} | S_0/S_{\text{tag}})) - \ln(LM(S_{\text{tag}} | S_0/S_{\text{tag}})) \| \\ &= \| \ln(\prod_{i=1}^n f(Y_i)) - \ln(\prod_{i=1}^n f(X_i)) \| \\ &= \| \sum_{i=1}^n \ln(f(Y_i)) - \sum_{i=1}^n \ln(f(X_i)) \| \\ &= \| \sum_{i=1}^n (\ln(f(Y_i)) - \ln(f(X_i))) \| \\ &\leq \sum_{i=1}^n \| \ln(f(Y_i)) - \ln(f(X_i)) \| \\ &< n \cdot \epsilon' = \epsilon, \end{aligned}$$

which completes the proof.

### C. Proof of Equation 6

For  $i = 1, \dots, \lambda$ , with Equation 4, we have

$$\| \ln(LM(S_i)) - \ln(LM(S_0)) \| \leq \epsilon.$$

For  $i = 0, \dots, \lambda$ , with Equation 5, we have

$$\| \ln(P(S_i)) - \ln(LM(S_i)) \| \leq \delta.$$

As a result, for  $i = 1, \dots, \lambda$ ,

$$\begin{aligned} &\| \ln(P(S_i)) - \ln(P(S_0)) \| \\ &= \| \ln(P(S_i)) - \ln(LM(S_i)) + \ln(LM(S_i)) - \ln(LM(S_0)) \\ &\quad + \ln(LM(S_0)) - \ln(P(S_0)) \| \\ &\leq \| \ln(P(S_i)) - \ln(LM(S_i)) \| + \| \ln(LM(S_i)) - \ln(LM(S_0)) \| \\ &\quad + \| \ln(LM(S_0)) - \ln(P(S_0)) \| \\ &\leq \delta + \epsilon + \delta = \epsilon + 2\delta, \end{aligned}$$

which implies Equation 6 and completes the proof.

#### D. Proof of Equation 7

As one of the  $\eta$  obtained prompts is the original prompt, let's assume  $idx_\eta = 0$ , that is,  $S_{idx_\eta} = S_0$ .

For  $j = 1, \dots, \eta - 1$ ,  $idx_j > 0$ . With Equation 6, we have

$$e^{-\epsilon-2\delta} P(S_0) \leq P(S_{idx_j}) \leq e^{\epsilon+2\delta} P(S_0).$$

As a result,

$$(1 + (\eta - 1)e^{-\epsilon-2\delta})P(S_0) \leq \sum_{j=1}^{\eta} P(S_{idx_j})$$

and

$$\sum_{j=1}^{\eta} P(S_{idx_j}) \leq (1 + (\eta - 1)e^{\epsilon+2\delta})P(S_0),$$

which implies Equation 7 and completes the proof.

#### E. Dataset Preparation for PO and Examples

Figure 12 is an example that illustrates the workflow of PO.

For the evaluation of PO, we selected the initial 500 entries from clinical dialogue datasets and 1500 entries from USMLE Step 2 passages. Since the initial datasets were not tagged with PII information, we used ChatGPT to automatically tag HIPAA-sensitive information according to the guidelines from [4], along with its PII category. Each entry in these datasets averaged 13 redacted PII segments. An example of a dataset item is shown in Figure 13. For the resume dataset, we extracted the first 1500 entries and used Google Cloud's PII filtering tool to annotate personal information, resulting in an average of 18 PII segments per entry. An anonymized example is presented in Figure 14.

*Example Output from GQS.* For demonstration, we present the result of running GQS on the name "Mrs. Loraine Wicks" in Figure 13, sampled with  $\epsilon = 1/32$  and  $\lambda_{\max} = 512$ . Due to space constraints, only the first 30 outputs are shown.

1) Mrs. Loraine Wicks	11) Mrs. Loraine Warner	21) Mrs. Lillian Winter
2) Mrs. Lillian Brown	12) Mrs. Lydia Martin	22) Mrs. Lillian Abraham
3) Mrs. Loraine Park	13) Mrs. Loraine Thompson	23) Mrs. Lillian Cooper
4) Mrs. Lydia Jackson	14) Mrs. Loraine Wood	24) Mrs. Lydia Davis
5) Mrs. Lydia Williams	15) Mrs. Loraine Brown	25) Mrs. Lillian Kim
6) Mrs. Lillian Thomas	16) Mrs. Lillian Grey	26) Mrs. Lillian Thompson
7) Mrs. Wilson	17) Mrs. Lillian Jenkins	27) Mrs. Lydia White
8) Mrs. Lydia Grant	18) Mrs. Lillian Watson	28) Mrs. Lillian Davis
9) Mrs. Lillian Taylor	19) Mrs. Lillian Anderson	29) Mrs. Lillian Carter
10) Mrs. Lydia Green	20) Mrs. Loraine Williams	30) Mrs. Loraine Miller



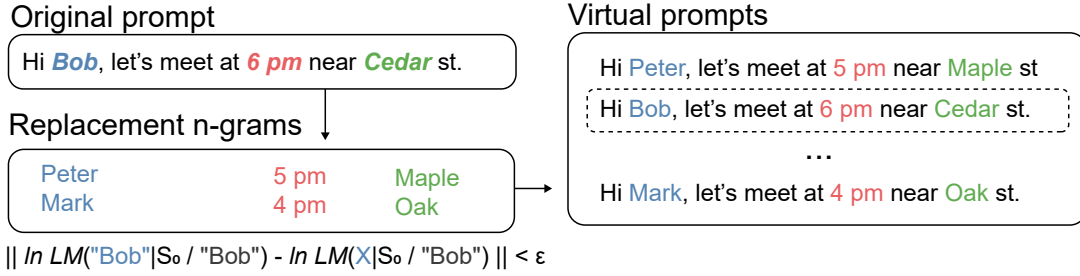


Fig. 12: **PO example**. Given a user prompt with tagged sensitive segments (e.g., names and addresses), PO samples replacement n-grams for each tagged segments using GQS. The sampled replacement n-grams are statistical indistinguishable from the original segment.

[AGE] 17-year-old [GENDER] male, has come to the [ORGANIZATION NAME] student health clinic complaining of [DISEASE] heart pounding. [PERSON NAME] Mrs. Loraine Wicks mother has given verbal consent for a history, physical examination, and treatment - began [DATES] 2-3 months ago, sudden, intermittent for [DATES] 2 days (lasting 3-4 min), worsening, non-allev/aggrav - associated with dyspnea on exertion and rest, stressed out about school - reports he feels like his heart is jumping out of his chest - ROS: denies chest pain, diaphoresis, weight loss, chills, fever, nausea, vomiting, pedal edema - PMH: none, meds: Adderall (from a friend), NKDA - FH: father had MI recently, mother has thyroid disease - SH: non-smoker, marijuana [DATES] 5-6 months ago, 3 beers on the weekend, basketball at school - SH: no STD.

Fig. 13: Example entry from the clinical dataset. Yellow-masked text indicates redacted information, with brackets denoting its PII category.

Resume Wizard [PERSON NAME] Jane Doe E-Mail: [EMAIL] jane.doe@example.com Phone: [ID] (123) 456-7890 (M) [ORGANIZATION NAME] Finance & Accounts, Costing Profile Introduction

- A dynamic professional with a qualitative experience of [AGE] 3 years 2 months in the areas of Finance & Accounts, Product Costing & MIS Reporting.
- Presently working as PROCESS LEAD at [ORGANIZATION NAME] Tech Solutions Inc.
- Previously worked as LEAD F&A OPERATIONS at [ORGANIZATION NAME] Global Tech with [ORGANIZATION NAME] Soft Drinks Co Project from [DATES] 1st April 2018 to [DATES] 30th June 2019.
- Involved in the standardization of process & MIS reporting files and contributed a higher rate of organic growth.
- An effective communicator with excellent relationship-building & interpersonal skills. Strong analytical, problem-solving & organizational abilities.
- Areas of interest include budgeting & preparation of AOP (Annual Operating Plans).
- Familiar with SAP FICO modules, MS Office tools.

Fig. 14: Example entry from the resume dataset. Note that we anonymized this example with placeholders such as “Jane Doe” and “(123) 456-7890” for privacy.